# Studies on Luminescence Properties of the Lanthanide Complexes Incorporated into Silica-based Glass Matrices

(シリカ基ガラスマトリックスに導入した希土類錯体の蛍光に関する研究)

**1997**

**Tetsuro Jin**

Department of Applied Chemistry
Faculty of Engineering
Osaka University

# Preface

The work of this thesis has been carried out under the guidance of Professor Dr. Gin-ya Adachi at Department of Applied Chemistry, Faculty of Engineering, Osaka University.

The object of this thesis is to elucidate the luminescence characteristics of europium (III) and terbium (III) complexes incorporated into silica-based glass matrices and to develop new red or green emitting photoluminescent devices.

The author wishes that results obtained in this study provide useful suggestion and information for further development of the photoluminescent phosphor using the lanthanide complexes, and that new lanthanide complex phosphors developed here are realized in practical use in near future.

Tetsuro Jin

Department of Applied Chemistry
Faculty of Engineering
Osaka University
Yamadaoka 2-1, Suita, Osaka 565
Japan

January 1997

# Contents

**Chapter 3**
**Photovoltaic Cell Characteristics of Hybrid Silicon Devices with Lanthanide Complex Phosphor Coating Film**

# General Introduction

The trivalent lanthanide ions have been known to give strong emissions under ultraviolet irradiation. The sharp luminescence transitions of the lanthanide ions correnspond to the absorption lines of the shielded 4f shell which is not entirely filled[1]. Consequently, compounds containing the optically active lanthanide ions, *e.g.* $Eu^{3+}$ and $Tb^{3+}$, have been used as phosphors and laser materials, for a long time, because of their sharp and intense emissions based on f-f electronic transitions. Among such trivalent lanthanides, $Eu^{3+}$ ion provides five narrow emission lines corresponding to a series of $^5D_0$ - $7F_i$ transitions, where i = 0, 1, 2, 3 and 4, and the strongest emission line assigned to the transition, $^5D_0$ - $^7F_2$, appears at about 610 nm[2-4]. In a similar manner as $Eu^{3+}$ ion, $Tb^{3+}$ ion has four narrow emission lines corresponding to $^5D_4$ - $^7F_j$ transitions, where j = 2, 3, 4 and 5, and the strongest line of $^5D_4$ - $^7F_5$ at 545 nm is observed as the green emission light with high purity[5].

On the other hand, the luminescence characteristics of the chelating lanthanide ions towards a variety of chelating ligands have been investigated. A particular complex may fluoresce owing to one of the following reasons: Emission may occur (1) from the excited ligand part of the molecule, perturbed by the metal ion, (2) from the excited metal ion perturbed by the ligand, and (3) due to the intramolecular energy transfer (IMET) process in the complexes, *i.e.* absorption of energy takes place in conjugated double bonds of the organic ligands and is transferred to the bound central metal ion (an indirect excitation of the metal ion) which in its turn may undergo a radiative transition, consequently giving rise to characteristic emission of the metal ion[6].

The lanthanide ions form stable crystalline complexes with heterocyclic ligands such as 2,2'-bipyridine (bpy) or 1,10-phenanthroline (phen) as shown in Fig. 1, which possess an excellent luminescence characteristics of them in the same mechanism as mentioned above[7-9]. However, the phosphors[10,11] and laser devices[12] made for the purpose of practical uses up to date are almost limited to inorganic solids. Therefore, the complexes or organic compounds containing lanthanide ions have been excluded from such applications because of their poor thermal, moisture

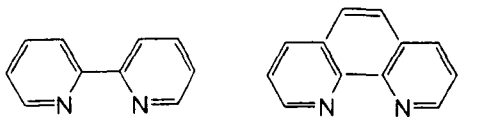

2,2'-Bipyridine ( bpy )  1,10-Phenanthroline ( phen )

**Figure 1.** Ligands used in this study.

stability attributed to deactivation by multiphonon relaxation and mechanical strength, although they also have good light-emitting characteristics for the uses of phosphors[13], laser devices[14,15] and biomimetic materials[16]. The emitting devices which possess a good luminescent property, however could be obtained when the lanthanide complexes are effectively incorporated into some solid state matrices in mild conditions.

Although the composite materials of the lanthanide complex incorporated into polymer matrices have been studied, in order to solve the above-mentioned problems[17], however, it is difficult to apply to materials such as phosphors from the reasons why most of plastics are considerably limited to be used as host matrices by their low photostability and poor thermal stability.

On the other hand, the sol-gel method can provide glasses and ceramics from viscous gel precurssors produced by polymerization of raw materials such as metal alkoxides under the much more gentle conditions than that of the conventional high-temperature melting technique[18,19] shown in following chemical reactions:

(1) Hydrolysis;

$$nSi(OC_2H_5)_4 + 4nH_2O \rightarrow nSi(OH)_4 + 4nC_2H_5OH$$

(2) Polymerization (Polycondensation);

$$nSi(OH)_4 \rightarrow nSiO_2 + 2nH_2O$$

Therefore, the sol-gel process has a great potential to provide unique inorganic light-emitting solid materials doped with organic compounds, *e.g.* phosphors[20], solid-state tunable dye laser media [21], and so on, which are typically incorporated into gel hosts via dissolution of the typically

active organic compounds into the initial precursor sol.

Furthermore, silica unit combined with monomer as an oligomeric unit into three-dimensional skeleton of silica, that is to say, organically modified silicate (ORMOSIL), has been synthesized and their physical characteristics have been studied by many scientists[22-27]. Advantages of these materials are 1) the preparation temperature is relatively low (< 150°C), 2) the density of resulting materials is high, 3) the obtained monolith is high transparency, 4) physical properties such as refractive index can be made-to-order by changing the chemical composition of gels, and 5) viscous liquids could be obtained, which allows bulk pieces to be molded or when diluted with a suitable solvent to be cast into thin films and fiber.

The present work deals with the elucidation and development of luminescence characteristics of trivalent europium and terbium complexes incorporated into silica-based glass matrices.

In Chapter 1, $[Ln(bpy)_2]Cl_3$ and $[Ln(phen)_2]Cl_3$ (Ln = Eu and Tb) were prepared and their luminescence properties were investigated. Consequently, silica-based composite materials, $SiO_2$:$[Ln(bpy)_2]^{3+}$ and $SiO_2$:$[Ln(phen)_2]^{3+}$ were prepared by sol-gel method, and their luminescence characteristics as well as thermal stability were studied.

Chapter 2 described that the silica-based ORMOSIL materials incorporated with two lanthanide complexes, $[Eu(phen)_2]Cl_3$ and $[Tb(bpy)_2]Cl_3$, which possessed an excellent luminescence intensity and heat-resistance property were prepared according to the sol-gel method. Furthermore, the luminescence properties of these lanthanide complexes and their ORMOSIL composite materials were investigated and their luminescence mechanisms were discussed.

In Chapter 3, the resulting composite materials described in Chapter 2 were able to transform the incident UV lights to visible ones, the outputs of solar batteries were demonstrated to be enhanced by simple surface coatings of them. The solar cell hybrid devices were fabricated by coating the ORMOSIL composite materials on the surface of amorphous (a-Si) or single crystal silicon (c-Si) solar cell panels, and their light transformation characteristics of sunlight to electric power were studied.

# List of Publication

[1] Luminescence Property of the Terbium Bipyridyl Complex Incorporated in Silica Matrix by a Sol-Gel Method

Tetsuro Jin, Shuji Tsutsumi, Yujiro Deguchi, Ken-ichi Machida, and Gin-ya Adachi

*Journal of the Electrochemical Society*, **142**, L195-L197 (1995).

[2] Preparation and Luminescence Characteristics of the Europium and Terbium Complexes Incorporated into a Silica Matrix Using a Sol-gel Method

Tetsuro Jin, Shuji Tsutsumi, Yujiro Deguchi, Ken-ichi Machida, and Gin-ya Adachi

*Journal of Alloys and Compounds*, in press (1996).

[3] Luminescence Characteristics of the Lanthanide Complex Incorporated into an ORMOSIL Matrix Using a Sol-gel Method

Tetsuro Jin, Shuji Tsutsumi, Yujiro Deguchi, Ken-ichi Machida, and Gin-ya Adachi

*Journal of the Electrochemical Society*, **143**, 3333-3335 (1996).

[4] High Conversion Efficiency Photovoltaic Cell Enhanced by Lanthanide Complex Phosphor Film Coating

Tetsuro Jin, Satoshi Inoue, Shuji Tsutsumi, Ken-ichi Machida, and Gin-ya Adachi

*Chemistry Letters*, in contribution.

[5] Luminescence Properties of Lanthanide Complexes into Sol-gel Derived Organic-inorganic Hybrid Materials

Tetsuro Jin, Satoshi Inoue, Shuji Tsutsumi, Ken-ichi Machida, and Gin-ya Adachi

Journal of the Non-crystalline Solids, in contribution.

[6] Photovoltaic Cell Characteristics of Hybrid Silicon Devices with Lanthanide Complex Phosphor Coating Film

Tetsuro Jin, Satoshi Inoue, Ken-ichi Machida, and Gin-ya Adachi

*Journal of the Electrochemical Society*, in preparation.

[7] Relationship between the Intramolecular Energy Transfer Efficiency and Triplet State Energy Level in Lanthanide Complexes

Tetsuro Jin, Satoshi Inoue, Ken-ichi Machida, and Gin-ya Adachi

*Journal of Luminescence*, in preparation.

# Chapter 1

## Preparation and Luminescence Characteristics of the Europium and Terbium Complexes incorporated into a Silica Matrix using a Sol-gel Method

### 1.1. Introduction

As mentioned in General Introduction, the photoactive lanthanide ions such as $Eu^{3+}$ and $Tb^{3+}$ could form stable crystalline complexes with heterocyclic ligands, *e.g.* 2,2'-bipyridine (bpy) and 1,10-phenanthroline (phen), which exhibit efficient energy transfer from the coordinated ligands to the chelated lathanide ions. The potential application feasibility of these compounds is based on the fact that the organic portion of molecules can absorb ultraviolet radiation and they provide sharp green line emissions with good efficiency via the subsequent intramolecular energy transfers. However, these lanthanide complexes themselves could not be used as emitting devices due to the poor stability of their luminescence in any conditions.

On the other hand, the silica glasses can be prepared via the sol-gel process at temperatures lower than that of the conventional melting method. Thus, the sol-gel process may be a suitable method for preparing a host matrix for photoactive compounds, such as organic metal complexes. In Chapter 1, the silica-based composite materials incorporated with the lanthanide bpy and phen complexes were prepared according to the sol-gel method and their luminescence property was studied together with their thermal stability.

### 1.2. Experimental details

### *1.2.1. Sample Preparation.*

The lanthanide phen complex was conventionally prepared by addition of 1,10-phenanthroline (99.9%, Wako Chemical Co., Ltd) to the ethanol solution containing the lanthanide chloride $LnCl_3 \cdot 6H_2O$, which was obtained by chlorination of lanthanide oxides ($Eu_2O_3$ or $Tb_4O_7$, 99.9 %, Shin-Etsu Chemical Co., Ltd.) with $NH_4Cl$ (99.9 %, Kanto Chemical Co., Ltd.) and these sample was especially used without further purification. After stirring overnight, the resulting white precipitate was filtrated. A hydrous complex $[Ln(phen)_2]Cl_3 \cdot 2H_2O$ was obtained from the solid by washing with ether and drying in vacuo at room temperature. The bpy complex was prepared by addition of 2,2'-bipyridyl (99.9 %, Wako Chemical) to the ethanol solution containing $LnCl_3$ in a similar manner as the $[Ln(phen)_2]Cl_3$ complex.

The appropriate amount of each the lanthanide complex was dissolved in the mixed solution of water, ethanol and tetraethoxysilane (TEOS, 99.9 %, Wako Chemical) with molar ratio of 11 : 7 : 1 by stirring thoroughly. In the case of our study, hydrochrolic acid or ammonia was not added because the sol solutions prepared here were sufficiently polymerized to gels without any catalyst. After aging at room temperature for 2 - 10 days, transparent gel solutions were formed and dried at 50 °C for several days. The final composite materials $SiO_2$:$[Ln(phen)_2]^{3+}$ and $SiO_2$:$[Ln(bpy)_2]^{3+}$ were obtained by heating at 100 - 600 °C for 5 h in air and grinding up to a particle size less than 50 μm by sieving them.

### *1.2.2. Measurement details.*

The resulting organolanthanide complexes and silica gel-based composite materials incorporated with them were identified on the basis of elemental analysis and IR absorption spectrum measurements. Thermogravimetric analysis (TG) of the lanthanide complexes and composite materials was performed up to 600 °C in air on a Rigaku thermal analysis apparatuses (Rigaku Theroflex TG 8110 and DSC 8240). The excitation and emission spectra were recorded on by a Hitachi-850 spectrofluorophotometer at room temperature. The sample was mounted in a

front face holder and the measurements were carried out under UV-visible excitation light. The relative emission intensity was calculated from the area of the emission spectrum recorded under an optimum excitation condition by normalizing that of $Y(P,V)O_4$:Eu or $LaPO_4$:Ce,Tb phosphor as 100 %. Measurements of IR spectra for the composite materials were made by using the conventional KBr pellet technique. Average error of the observational values in this work was less than 3 %.

## 1.3. Results

### *1.3.1. Europium complexes and their composite materials.*

Excitation and emission spectra of $[Eu(bpy)_2]Cl_3 \cdot 2H_2O$ complex was shown in Figure 1.1, together with the excitation spectrum of $EuCl_3$. Although an original absorption band ($^7F_0$ - $^5L_6$ transition) of $Eu^{3+}$ ion was usually observed at around 394 nm , such absorption scarecely reflected on the excitation spectrum of the $[Eu(bpy)_2]Cl_3 \cdot 2H_2O$ complex and the broad and wide absorption

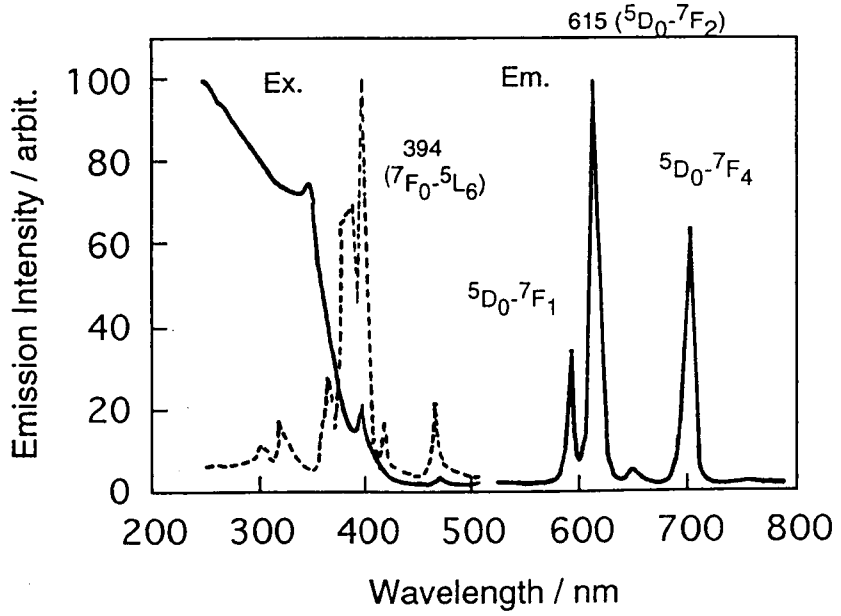


**Figure 1.1.** Excitation and emission spectra of $[Eu(bpy)_2]Cl_3 \cdot 2H_2O$ (solid line) and $EuCl_3$ (dashed line).

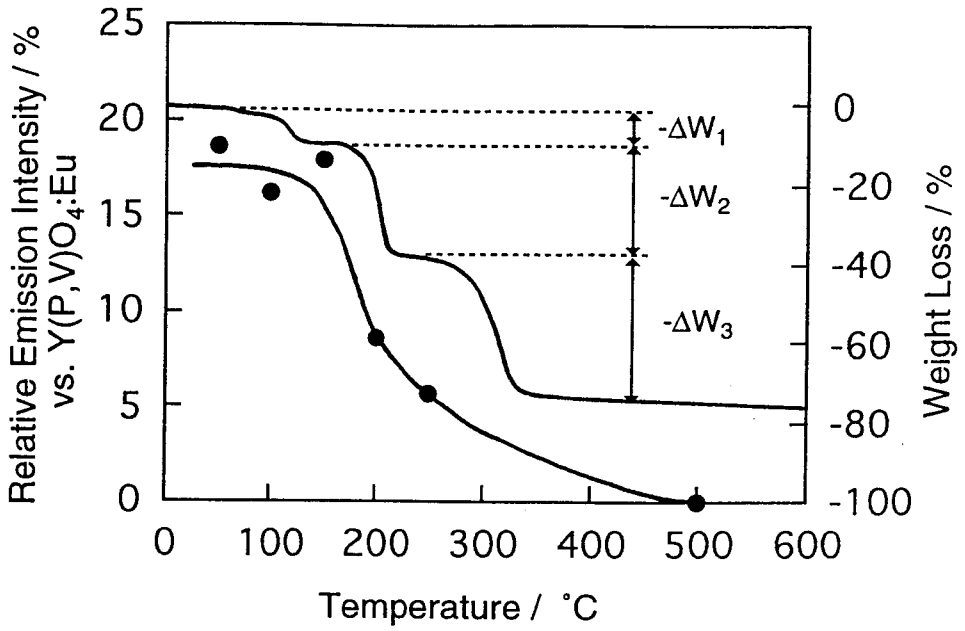


**Figure 1.2.** Temperature dependences of the relative emission intensity and weight loss (TG curve) for $[Eu(bpy)_2]Cl_3 \cdot 2H_2O$. Heating rate for TG, $5^{\circ}C min^{-1}$.

curve was dominated by band at about 340 nm. This band is assignable to the efficient $\pi$ - $\pi^*$ transition based on the conjugated double bond of bpy ligand. Consequently, the strong red emission can be observed from the chelated $Eu^{3+}$ ion via the efficient energy transfer from the surrounding bpy ligands. In the case of $EuCl_3$, however, the emission intensity was considerably weaker than that of $[Eu(bpy)_2]Cl_3$ complex itself because no such energy transfer takes place.

Figure 1.2 shows temperature dependences for the weight loss (TG) and relative emission intensity of the original $[Eu(bpy)_2]Cl_3 \cdot 2H_2O$ complex. The initial weight loss in a region of $-\Delta w_1$ started at 100 °C was 6.7 % and was assignable to the loss of solvated water. The second and third ones in regions of $-\Delta w_2$ and $-\Delta w_3$ at 200 - 300 °C were ca. 30 %, respectively. These reductions were caused by the elimination and/or decomposition of bpy ligands. At the temperature above 330 °C, $[Eu(bpy)_2]Cl_3 \cdot 2H_2O$ was completely decomposed to EuClO. The relative emission intensity of $[Eu(bpy)_2]Cl_3 \cdot 2H_2O$ kept a constant up to ca. 150 °C but it was drastically decreased by the heat treatment above this temperature. This is due to the decomposition of $[Eu(bpy)_2]Cl_3$ itself by the elimination and/or decomposition of ligands. On the other hand, the europium β-diketone complexes such as $[Eu(acac)_3] \cdot nH_2O$ also provide strong emission spectra, but they were decomposed only by heating around 100 °C.

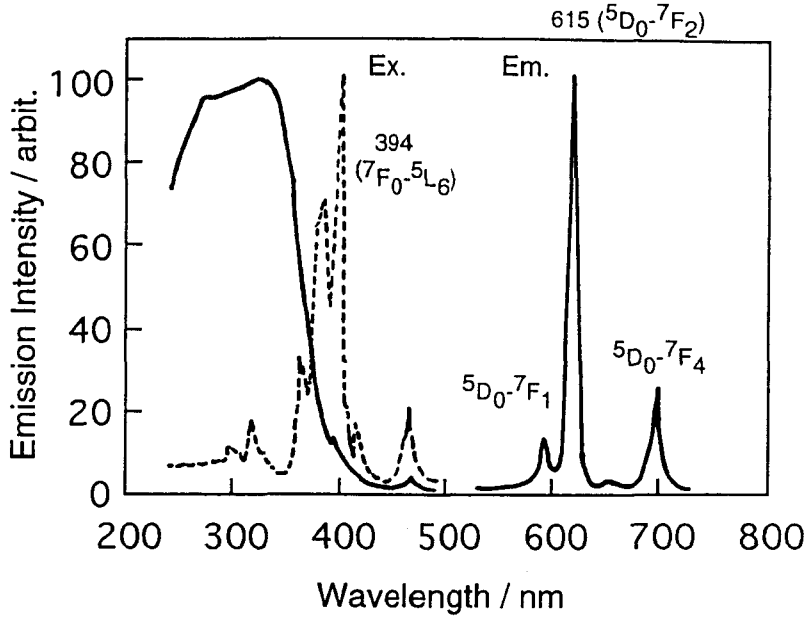


**Figure 1.3.** Excitation and emission spectra of $[Eu(phen)_2]Cl_3 \cdot 2H_2O$ (solid line) and the complex after heat treatment at 600°C (dashed line).

Excitation and emission spectra of the $[Eu(phen)_2]Cl_3 \cdot 2H_2O$ complex heated at 150 °C are shown in Figure 1.3, together with the excitation spectrum of $EuCl_3$. The excitation spectrum was observed as a broad band peaking at ca. 330 nm and the strong emission spectrum consisted of three main lines at 590 nm ($^5D_0$ - $^7F_1$), 615 nm ($^5D_0$ - $^7F_2$) and 700 nm ($^5D_0$ - $^7F_4$) based on $Eu^{3+}$ ion. As well as the case of $[Eu(bpy)_2]Cl_3$ complex, the absorption at 330 nm is due to the $\pi$ - $\pi^*$ transition of phen ligand. This means that the energy transfer occurs from the phen ligand to $Eu^{3+}$ ion. For the complex heated at 350 °C, however, the broad band disappeared in the excitation spectrum and the corresponding three emission lines were also weakened. This indicates that most of the $[Eu(phen)_2]Cl_3 \cdot 2H_2O$ complex was completely decomposed and hence the emission intensity was decreased.

Figure 1.4 shows temperature dependences of the weight loss and relative emission intensity of original $[Eu(phen)_2]Cl_3 \cdot 2H_2O$ complex. The initial weight loss in a region of $-\Delta w_1$ of $[Eu(phen)_2]Cl_3 \cdot 2H_2O$ at 100 °C was about 6.3 %. This is assignable to the vaporization of solvated water from the complex. The large weight loss in a region of $-\Delta w_2$ as started at about 300 °C was evaluated to ca. 60 % of which the value was attributed to the elimination and/or decomposition of

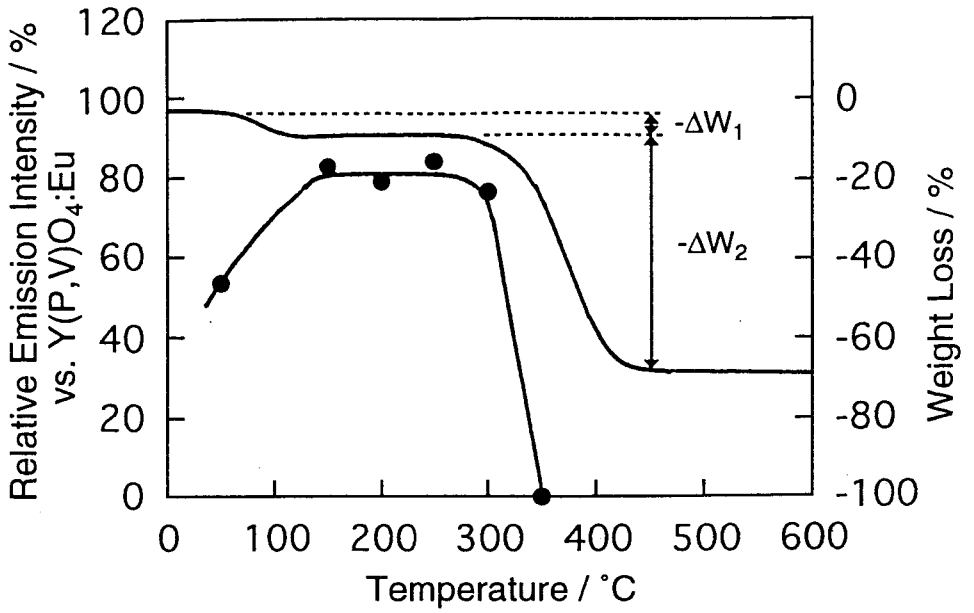


**Figure 1.4.** Temperature dependences of the relative emission intensity and weight loss (TG curve) for $[Eu(phen)_2]Cl_3 \cdot 2H_2O$. Heating rate for TG, 5°Cmin$^{-1}$.

phen ligand as well as $[Eu(bpy)_2]Cl_3 \cdot 2H_2O$. Above 350 °C, the complex was completely decomposed. The relative emission intensity of $[Eu(phen)_2]Cl_3 \cdot 2H_2O$ complex was increased with elevating the heat temperature up to 150 °C and a maximum value of ca. 80 % was obtained at this temperature. This indicated that the material derived from $[Eu(phen)_2]Cl_3 \cdot 2H_2O$ is also a good phosphor with the comparable luminescent ability to $Y(P,V)O_4$:Eu which is used as the lamp phosphor. Furthermore, from the result that this maximum value was maintained up to about 300 °C, it was concluded that the material derived from $[Eu(phen)_2]Cl_3$ complex possesses a good thermal stability. However, the emission intensity was decreased with elevating heat temperature up to 350 °C, and finally the complex was decomposed completely and only the weak emission spectrum similar to that of $EuCl_3$ was observed as mentioned above. This result is due to the decomposition and/or elimination of phen ligands in the above temperature region as supported by the TG data that $[Eu(phen)_2]Cl_3 \cdot 2H_2O$ complex is completely decomposed at 350 °C.

A series of IR spectrum patterns observed on the $[Eu(bpy)_2]Cl_3 \cdot 2H_2O$ complex and $SiO_2$:$[Eu(bpy)_2]^{3+}$ composite materials are shown in Figure 1.5. For $SiO_2$:$[Eu(bpy)_2]^{3+}$ composite materials, additional absorption peaks in regions of A (C=C and C=N stretch) and B (C-H out of plane bend) were superimposed on the original pattern of $SiO_2$ and their intensity was enhanced

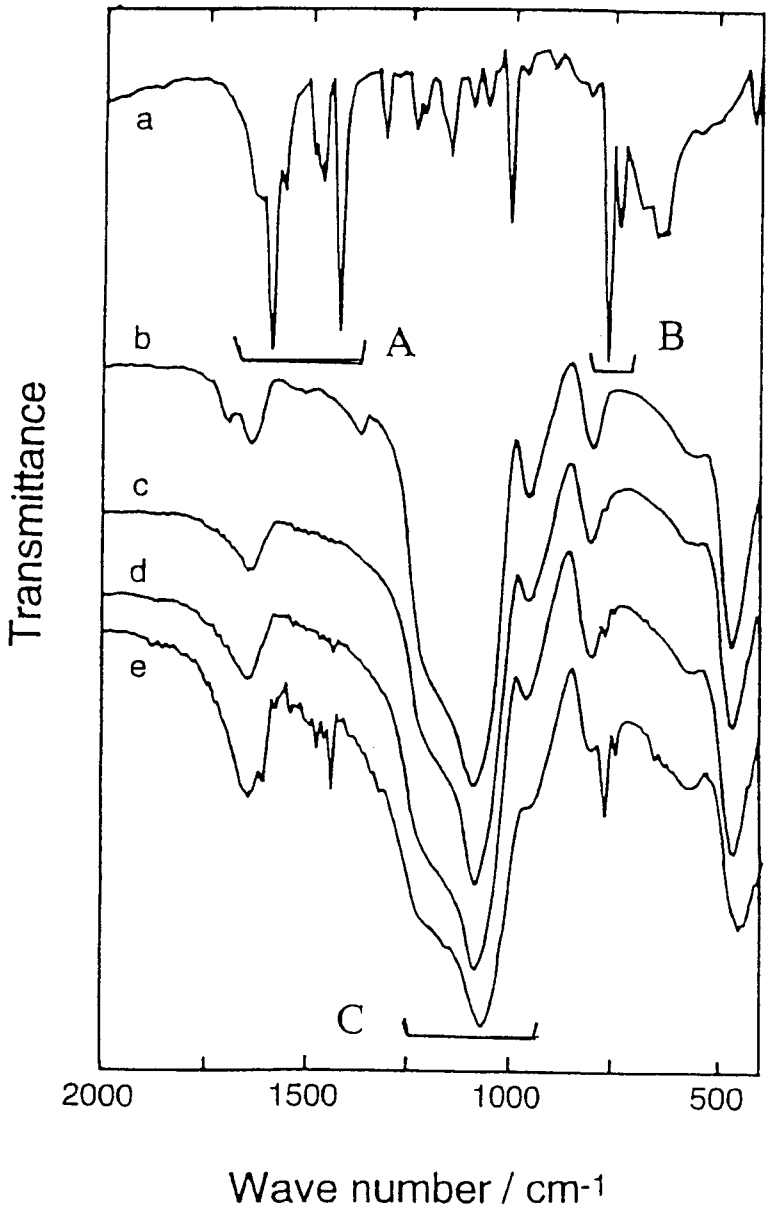


**Figure 1.5.** IR spectra of (a) the original $[Eu(bpy)_2]Cl_3 \cdot 2H_2O$ complex, and (b-e) $SiO_2$:$[Eu(bpy)_2]^{3+}$ (x mol%) composite materials with various concentrations x of $[Eu(bpy)_2]^{3+}$: (b), x = 0 ($SiO_2$ alone), (c) x = 1, (d) x = 3, and (e) x = 10. Heat treatment: in air, 250°C, 5h.

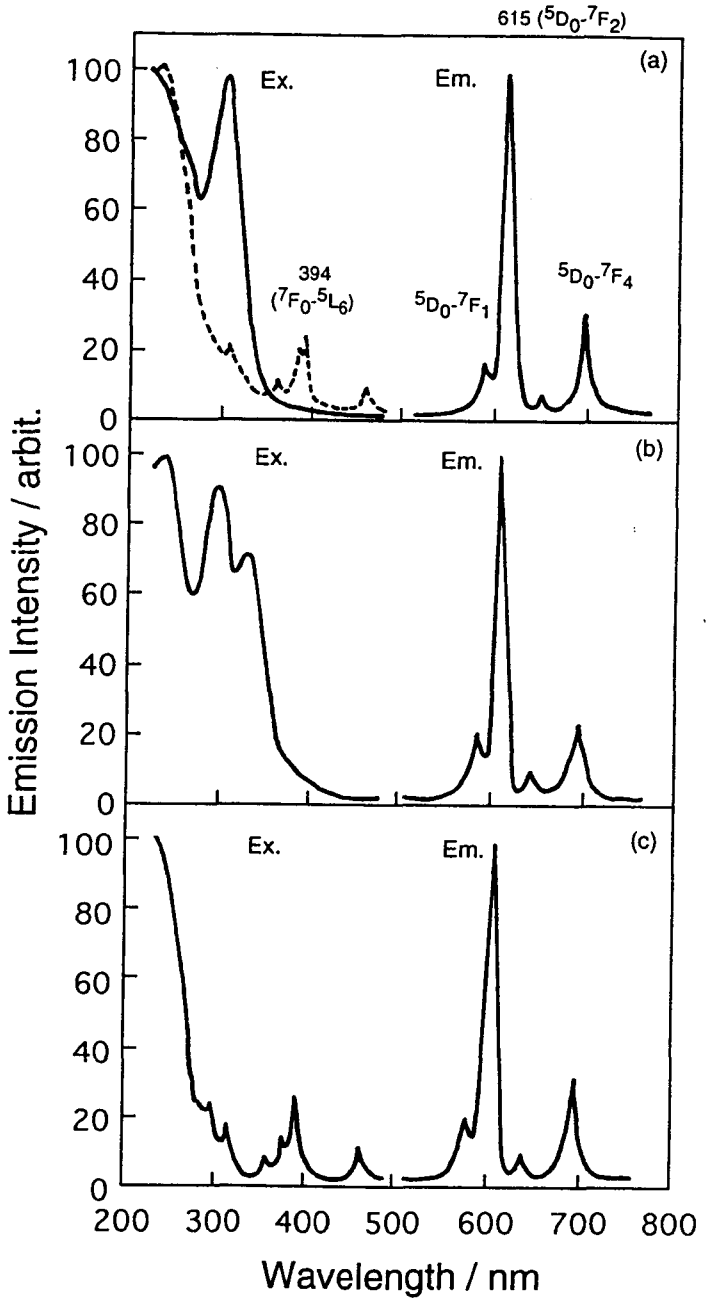


**Figure 1.6.** Excitation and emission spectra of $SiO_2$:$[Eu(bpy)_2]^{3+}$ (1 mol%) composite materials heated at various temperatures for 5h in air: (a) 250°C, (b) 450°C, and (c) 600°C.

with increasing the concentration of $[Eu(bpy)_2]Cl_3$, although the $SiO_2$ matrix provided a simple strong absorption band based on the Si-O stretch in a wavenumber region of C. This indicates that the $[Eu(bpy)_2]Cl_3$ complex is incorporated into the $SiO_2$ matrix without any decomposition or serious modification according to the nominal concentration of complex. However, the uniform and transparent material of $SiO_2$:$[Eu(bpy)_2]^{3+}$ was not obtained from the sol solution containing the larger amount of $[Eu(bpy)_2]Cl_3$ than 10 mol%. This is due to the segregation of these lanthanide complex in the silica matrix. When the concentration of the $[Eu(phen)_2]Cl_3 \cdot 2H_2O$ complex in the silica matrix was below 3 mol%, the $SiO_2$:$[Eu(bpy)_2]^{3+}$ composite materials with good transparency and uniformity were obtained with good reproducibility. The same results as the $[Eu(bpy)_2]Cl_3 \cdot 2H_2O$ complex and its composite materials were also observed on the $[Eu(phen)_2]Cl_3 \cdot 2H_2O$ and its derivatives.

Excitation and emission spectra of the composite materials doped with 1 mol% of the $[Eu(bpy)_2]Cl_3 \cdot 2H_2O$ complex [$SiO_2$:$[Eu(bpy)_2]^{3+}$ (1 mol%)] as heated at 150, 450 and 600 °C are shown in Figure 1.6. The emission profile measured was closely similar to that emission spectrum of the original $[Eu(bpy)_2]Cl_3 \cdot 2H_2O$ complex itself: The red emission spectra were observed even on the composite materials incorporated with a small amount of $[Eu(bpy)_2]Cl_3 \cdot 2H_2O$, such as $SiO_2$:$[Eu(bpy)_2]^{3+}$ (0.1 mol%), and were assigned to the $[Eu(bpy)_2]^{3+}$ complex cation incorporated into the silica matrix (see Figs. 6a and 6b). Particularly, the fact that the absorption band based on the $\pi$ - $\pi^*$ band also reflects to the excitation spectrum pattern indicates that the $[Eu(bpy)_2]^{3+}$ complex cations exist into the $SiO_2$ matrix and they maintain the original molecular composition and structure. Furthermore, the strong red emission was still observed on the $SiO_2$:$[Eu(bpy)_2]^{3+}$ composite material heated at the higher temperature than that at which the $[Eu(bpy)_2]Cl_3 \cdot 2H_2O$ complex was almost decomposed (> 180 °C). This means that the thermal stability of $[Eu(bpy)_2]Cl_3 \cdot 2H_2O$ is improved by the incorporation into the silica gel matrix. However, the excitation spectrum based on the bpy ligand at ca. 310 - 330 nm disappeared by the heat treatment at 600 °C. Consequently, the emission spectra of the composite materials were significantly weakened compared with that of the sample heated up to 450 °C and only weak emission lines ascribed to the free $Eu^{3+}$ ion derived via the decomposition of complex were observed (see Fig. 6c).

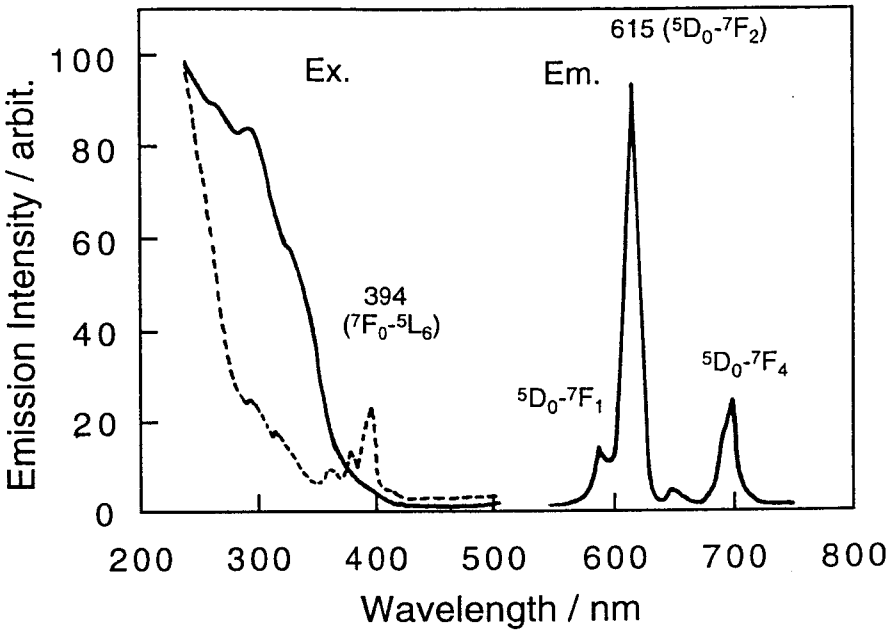


**Figure 1.7.** Excitation and emission spectra of $SiO_2$:$[Eu(phen)_2]^{3+}$ (1 mol%) (solid line) and $SiO_2$:$Eu^{3+}$ (dashed line) composite materials.

The $SiO_2$:$[Eu(phen)_2]^{3+}$ (1 mol%) composite materials also provided the excitation and emission spectra somewhat different from the $SiO_2$:$[Eu(bpy)_2]^{3+}$ composite materials (see Figure 1.7). The excitation spectrum pattern consisted of the broad decline curve with several shoulder peaks and the shape was similar to that of the original $[Eu(bpy)_2]Cl_3 \cdot 2H_2O$ complex rather than the $[Eu(phen)_2]Cl_3 \cdot 2H_2O$ one. In addition, the relative emission intensity of $SiO_2$:$[Eu(phen)_2]^{3+}$ was greater than that of $SiO_2$:$[Eu(bpy)_2]^{3+}$. This is due to the efficient $\pi$ - $\pi^*$ transition from the phen ligand to the chelated $Eu^{3+}$ ion, indicating that the $[Eu(phen)_2]Cl_3 \cdot 2H_2O$ complex is incorporated into the silica gel matrix with maintaining its original molecular structure which contributes to the strong emission.

Heat treatment temperature dependences of the $SiO_2$:$Eu^{3+}$ and the $SiO_2$:$[Eu(bpy)_2]^{3+}$ composite materials with various concentration of complex are shown in Figure 1.8. The relative emission intensities of the $SiO_2$:$[Eu(bpy)_2]^{3+}$ composite materials were higher than that of the $SiO_2$:$Eu^{3+}$ material. In the case of the composite materials doped with 0.1 and 1 mol% of

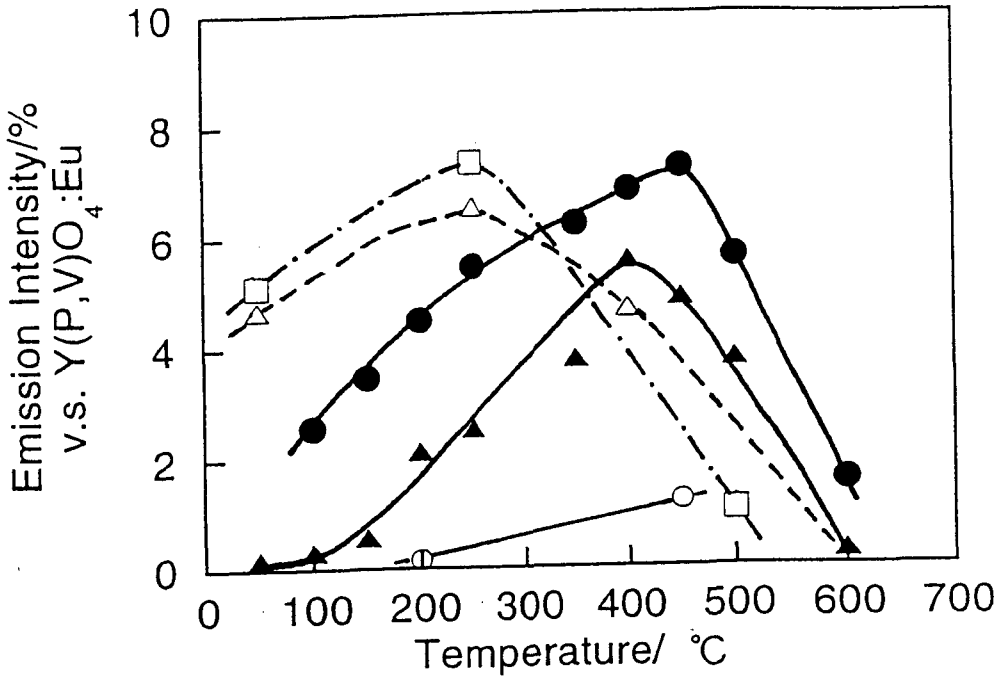


**Figure 1.8.** Temperature dependences of the relative emission intensities of $SiO_2$:$Eu^{3+}$ (0.1 mol%) (○) and $SiO_2$:$[Eu(bpy)_2]^{3+}$ (x mol%) with various concentration values x of $[Eu(bpy)_2]^{3+}$: x = 0.1 (▲), x = 1 (●), x = 3 (△), and x = 10 (□). Heat treatment: in air, 5h.

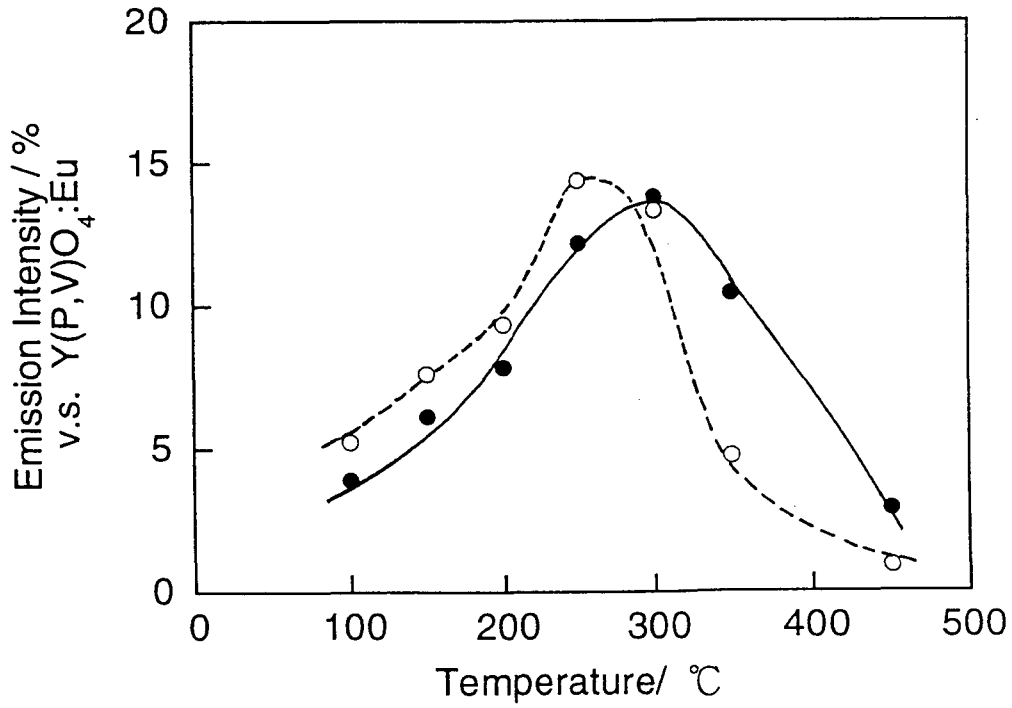


**Figure 1.9.** Temperature dependences of the relative emission intensities of $SiO_2$:$[Eu(phen)_2]^{3+}$ (x mol%) with two concentration values x of $[Eu(phen)_2]^{3+}$: x = 1 (●), and x = 3 (○). Heat treatment: in air, 5h.

$[Eu(bpy)_2]Cl_3 \cdot 2H_2O$, the relative intensity was maximized by the heat temperatures at the relative high temperature of 400 - 460 °C. Therefore, the resulting $SiO_2$:$[Eu(bpy)_2]^{3+}$ composite materials incorporated with ~ 1 mol% of $[Eu(bpy)_2]Cl_3 \cdot 2H_2O$ were concluded to possess a good thermal stability. Particularly, since the lanthanide complex incorporated into the silica gel matrix was effectively protected from the moisture by the surrounding $SiO_2$ units, their luminescence property was very stable after the standing in air. The emission intensity of $SiO_2$:$[Eu(bpy)_2]^{3+}$ was increased with the amount of complex to incorporate, e.g. 6.5 and 7.5 % for the samples with x = 3 and 10 mol% (treatment temperature = 250 °C), the thermal stability became poor with increasing of the concentration of $[Eu(bpy)_2]Cl_3 \cdot 2H_2O$ beyond x = 3 because the excess amount of $[Eu(bpy)_2]Cl_3 \cdot 2H_2O$ complex was segregated in the boundary of $SiO_2$ matrix grains.

Figure 1.9 shows the heat treatment temperature dependences of the emission intensity for $SiO_2$:$[Eu(phen)_2]^{3+}$ composite materials. In the low temperature region, the emission intensity of complexes was increased with elevating temperature for heat treatments as well as the original $[Eu(phen)_2]Cl_3 \cdot 2H_2O$ complex and the $SiO_2$:$[Eu(phen)_2]^{3+}$ composite materials. This is also due to the removal of solvated water from both the complex and silica matrix. The emission intensity for each composite materials (1 mol%) was maximized at 250 - 300 °C, providing a relative intensity value of about 15 %. It is noted that the specific intensity value per complex formula unit for the $SiO_2$:$[Eu(bpy)_2]^{3+}$ is several times higher than that of the original $[Eu(phen)_2]Cl_3 \cdot 2H_2O$ complex.

### *1.3.2. Terbium complex and their composite materials.*

Excitation and emission spectra of $[Tb(bpy)_2]Cl_3 \cdot 2H_2O$ complex are shown in Figure1.10. The excitation spectrum for $[Tb(bpy)_2]Cl_3 \cdot 2H_2O$ complex consisted of the broad curve with a shoulder peak at ca. 340 nm as assigned to the $\pi$ - $\pi^*$ absorption of bpy ligands, and thus the strong green emission of $Tb^{3+}$ ion was observed via the energy transfer. The complex residue heated at 600 °C only showed the simple excitation spectrum based on the unchelated $Eu^{3+}$ ion, and hence the corresponding five emission lines were considerably weakened.

Temperature dependences of the weight loss and emission intensity of the original

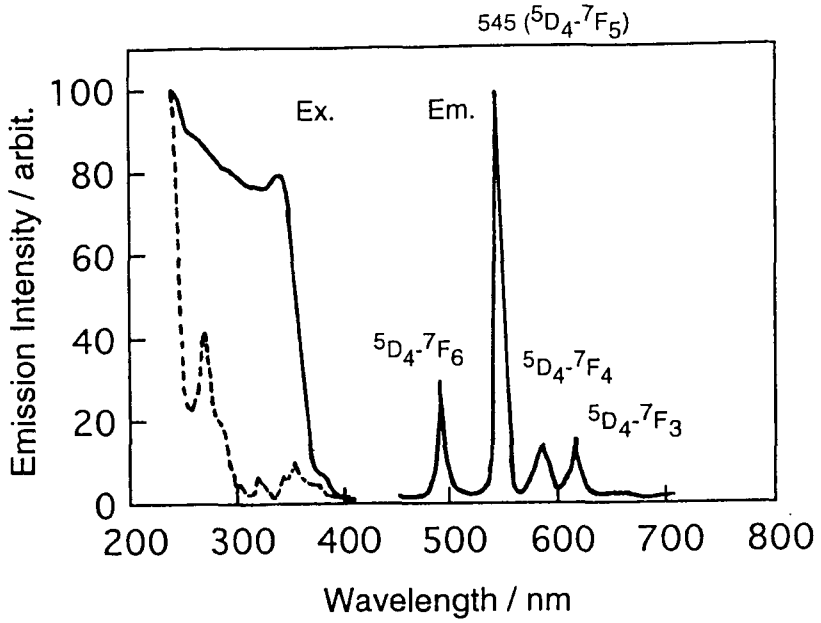


**Figure 1.10.** Excitation and emission spectra of the $[Tb(bpy)_2]Cl_3 \cdot 2H_2O$ complex (solid line) and $TbCl_3$ (dashed line).

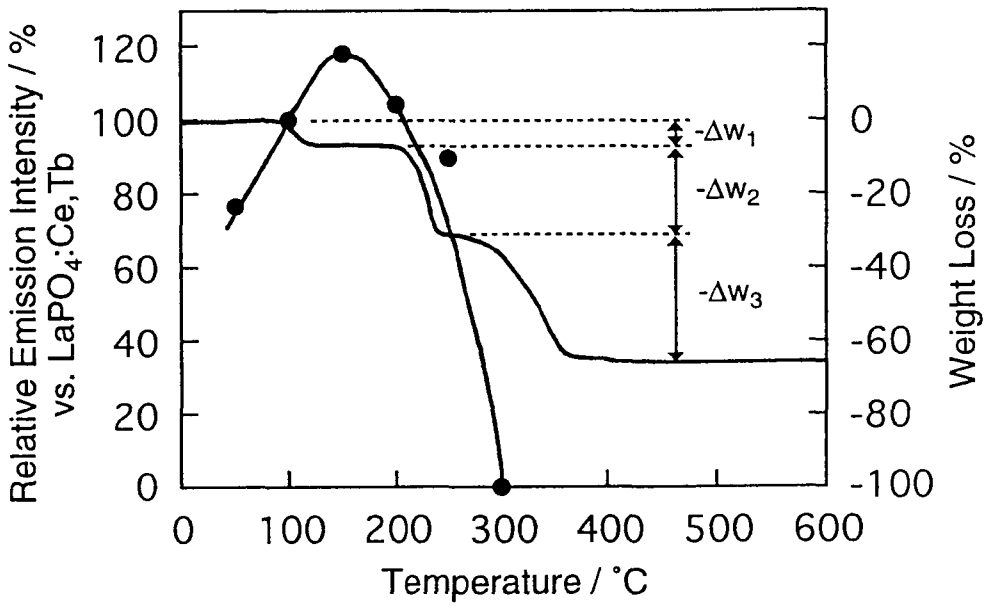


**Figure 1.11.** Temperature dependences of the relative emission intensity and weight loss (TG curve) for $[Tb(bpy)_2]Cl_3 \cdot 2H_2O$. Heating rate for TG, 5°Cmin$^{-1}$.

$[Tb(bpy)_2]Cl_3 \cdot 2H_2O$ complex are shown in Figure 1.11. The first weight loss was observed at about 100 °C and the value was estimated to about 6.3 %. This is due to the vaporization of solvated water. The weight loss values in second and third steps observed at 200 - 350 °C, $-\Delta w_2$ and $-\Delta w_3$, were approximately 30 % and attributed to the elimination and/or decomposition of bpy ligands in a similar manner as the case of $[Eu(bpy)_2]Cl_3 \cdot 2H_2O$. Above 350 °C, the $[Tb(bpy)_2]Cl_3 \cdot 2H_2O$ com-

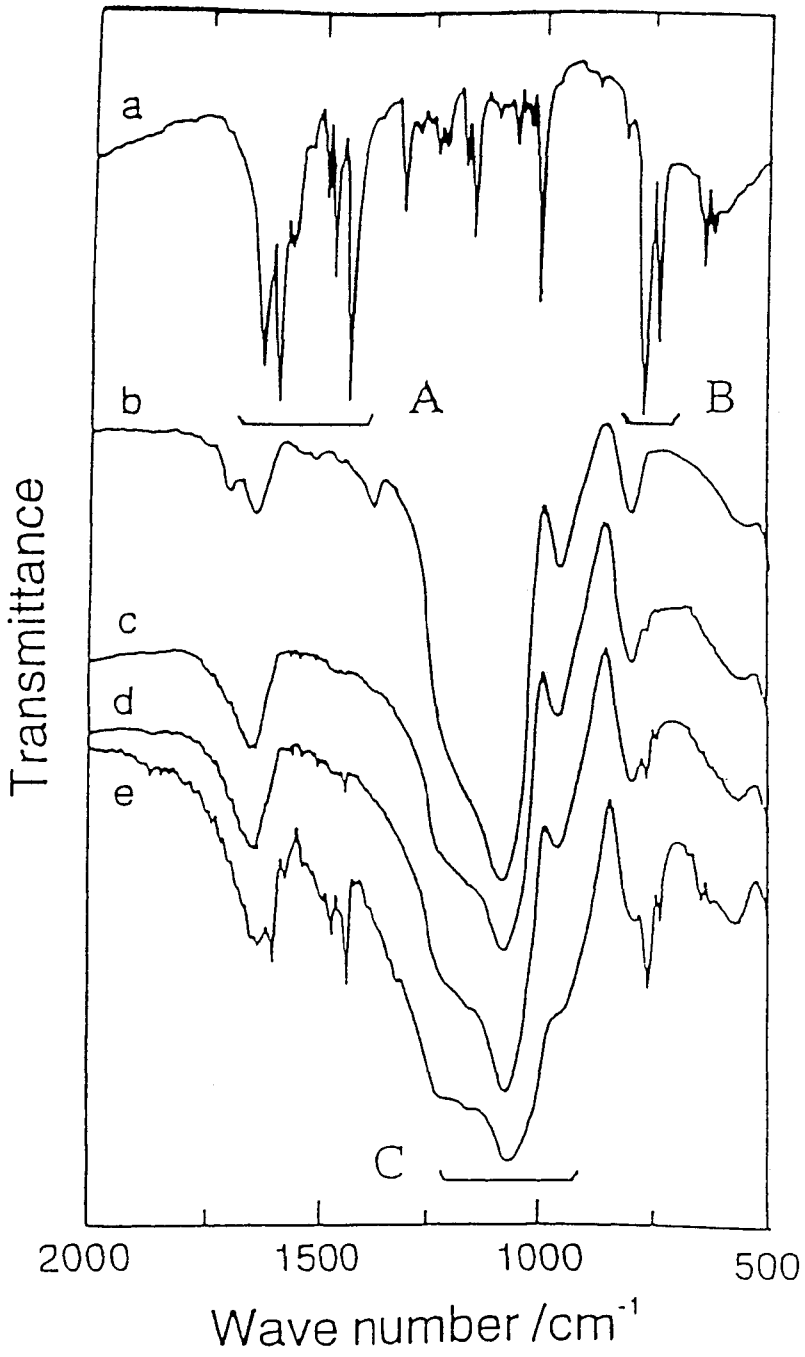


**Figure 1.12.** IR spectra of (a) the original $[Tb(bpy)_2]Cl_3 \cdot 2H_2O$ complex and (b-e) $SiO_2$:$[Tb(bpy)_2]^{3+}$ (x mol%) composite materials with various contents x of $[Tb(bpy)_2]^{3+}$: (b) x = 0 ($SiO_2$ alone), (c) x = 1, (d) x = 3, and (e) x = 10. Heat treatment: in air, 250°C, 5h.

plex was completely decomposed because any weight loss was no longer observed even in the higher temperature region.

On the other hand, an interesting behavior of emission intensity was observed on $[Tb(bpy)_2]Cl_3 \cdot 2H_2O$. The relative emission intensity of $[Tb(bpy)_2]Cl_3 \cdot 2H_2O$ was significantly increased with temperature for the heat treatment up to 150 °C, and the relative intensity evaluated against that of $LaPO_4$:Ce,Tb as used as a standard phosphor attained the highest value of 112.7 % (see Figure 1.11). This surprising enhancement of emission intensity may be due to the elimination of solvated water which inhibits the energy transfer via the $\pi$ - $\pi^*$ transition of bpy ligand to the lanthanide ion. Above 150 °C, however, the emission intensity was significantly depressed because of the elimination and/or decomposition of bpy ligands. The elimination of one ligand in $[Tb(bpy)_2]Cl_3$ complex takes place at 300 °C and this destruction of the molecular structure is responsible for the steep decrease in emission intensity.

A series of IR spectrum patterns observed on the $[Tb(bpy)_2]Cl_3 \cdot 2H_2O$ and $SiO_2$:$[Tb(bpy)_2]^{3+}$ composite materials are shown in Figure 1.12. In analogy with the case of $[Eu(bpy)_2]Cl_3$ complex, the absorption peaks assign to the terbium bpy complex, C=N and C=C stretch in the region A and C-H out of plane bending in the region B, were intensified with increase of the amount of complex, apart from the Si-O stretch in a wavenumber region C. However, the uniform and transparent material of $SiO_2$:$[Tb(bpy)_2]^{3+}$ was not obtained from the mixture containing the larger amount of $[Tb(bpy)_2]Cl_3 \cdot 2H_2O$ more than 10 mol%.

Excitation and emission spectra of the $SiO_2$:$[Tb(bpy)_2]^{3+}$ (1 mol%) composite material heated at 150, 300 and 600 °C are shown in Figure 1.13, together with that of $SiO_2$:$Tb^{3+}$. The shoulder peaks at about 310 nm as observed on the excitation spectra of the $SiO_2$:$[Tb(bpy)_2]^{3+}$ composite materials heated to 150 and 300 °C (see Figures 1.13a and 1.13b), assigned to the $\pi$ - $\pi^*$ transition of the bpy ligand. Therefore, it is concluded that the chelated $Tb^{3+}$ ions, that is, the $[Tb(bpy)_2]Cl_3$ complex still exist in the silica matrix prepared via the sol-gel process and the same molecular structure as the original $[Tb(bpy)_2]Cl_3 \cdot 2H_2O$ complex was maintained even after heat treatment up to 300 °C. However, the composite material heated to 600 °C provided no shoulder band at about 310 nm on the excitation. This means that the $[Tb(bpy)_2]^{3+}$ complex is also decomposed at 600 °C.

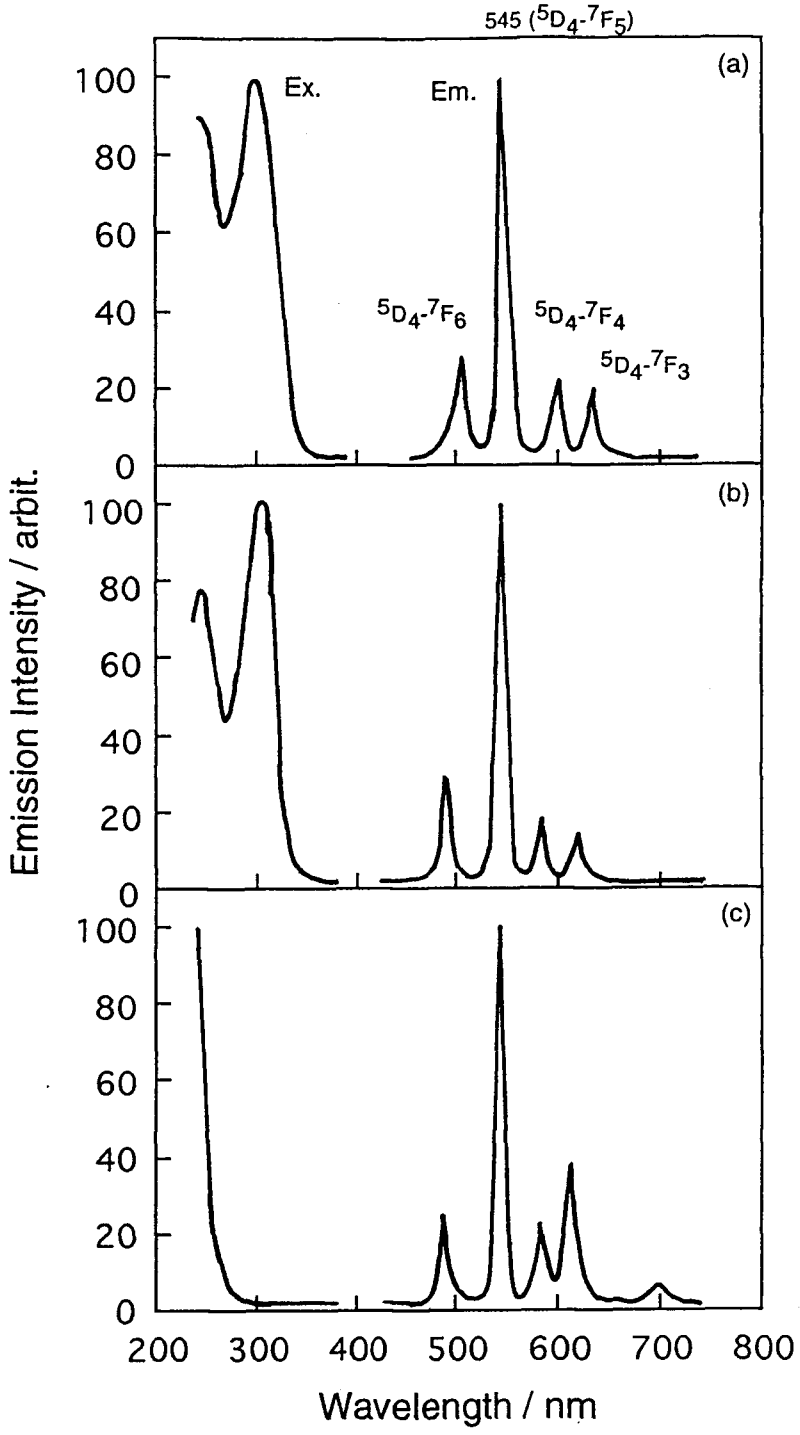


**Figure 1.13.** Excitation and emission spectra of $SiO_2$:$[Tb(bpy)_2]^{3+}$ (1 mol%) composite materials heated at various temperatures for 5 h in air: (a) 150°C, (b) 300°C, and (c) 600 °C.

The emission spectrum pattern of $SiO_2$:$[Tb(bpy)_2]^{3+}$ composite materials consisted of four main lines at 489 nm ($^5D_4$ - $^7F_6$), 545 nm ($^5D_4$ - $^7F_5$), 586 nm ($^5D_4$ - $^7F_4$) and 622 nm ($^5D_4$ - $^7F_3$), and among them the emission line at 545 nm was the strongest. The emission intensities of $SiO_2$:$[Tb(bpy)_2]^{3+}$ composite materials were considerably greater than those of $TbCl_3$ and $SiO_2$:$Tb^{3+}$ (doped with $TbCl_3$). However, the emission intensity for the composite material heated to 600 °C decreased to the same level as that of $SiO_2$:$Tb^{3+}$ and there was no contribution to the energy transfer between the bpy ligand and the $Tb^{3+}$ ion. These results indicate that the energy transfer from the bpy ligand to the chelated $Tb^{3+}$ ion is essential to enhancement of the emission intensity of $Tb^{3+}$ ion.

The relationships between the treatment temperature and emission intensity for $SiO_2$:$[Tb(bpy)_2]^{3+}$ and $SiO_2$:$[Tb(phen)_2]^{3+}$ composite materials are shown in Figure 1.14. In the lower temperature region, the emission intensities of terbium complexes were increased with temperature for the heat treatment by incorporating them to the silica matrix. This is due to the dehydration from both the complexes and silica matrix, which contributes to depress the non-

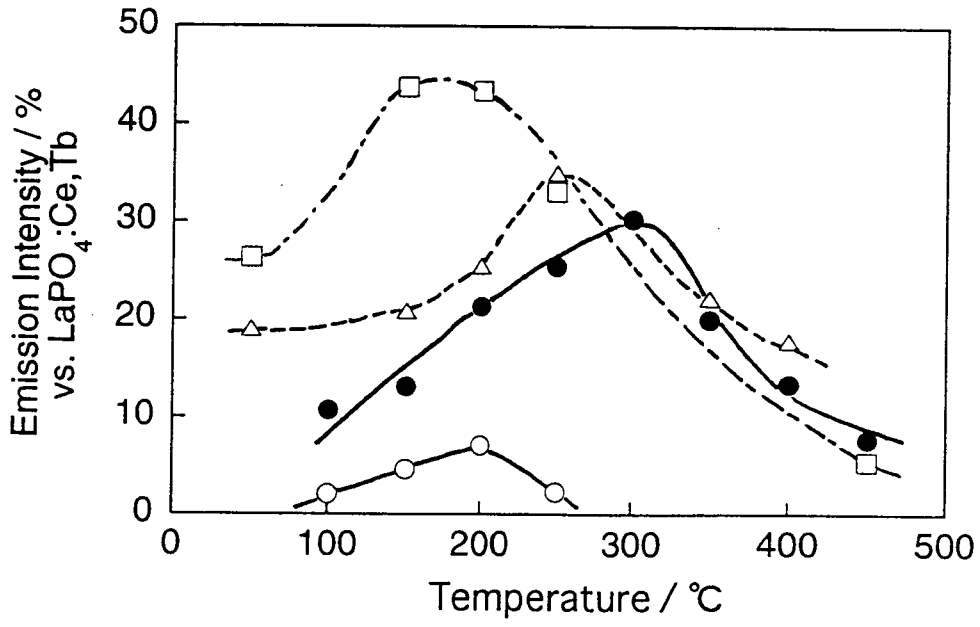


**Figure 1.14.** Temperature dependences of the relative emission intensities of $SiO_2$:$[Tb(phen)_2]^{3+}$ (1 mol%) (○) and $SiO_2$:$[Tb(bpy)_2]^{3+}$ (x mol%) with various concentration values x of $[Tb(bpy)_2]^{3+}$: x = 1 (●), x = 3 (△), and x = 10 (□). Heat treatment: in air, 5 h.

radiative process via water. The emission intensity for the composite material incorporated with 1 mol% of the bpy complex, $SiO_2$:$[Tb(bpy)_2]^{3+}$ (1 mol%) was maximized at 300 °C, indicating that the thermal stability of $[Tb(bpy)_2]Cl_3 \cdot 2H_2O$ was improved by surrounding with $SiO_2$ units in a similar manner as $SiO_2$:$[Eu(bpy)_2]^{3+}$. Especially, the emission intensity of the $SiO_2$:$[Tb(bpy)_2]^{3+}$ (1 mol%)

composite material was maximized at 300 °C and provided the value of 44 %. It is concluded from this value that the specific emission intensity value per $[Tb(bpy)_2]Cl_3$ formula unit is several decade times higher than that of the original complex. In addition, the mechanical properties of lanthanide complexes were improved by incorporation into the silica matrix. However, the emission intensity was also decreased by the heat treatment above 300 °C.

### 1.4. Discussion

The heat-resistance temperature of $[Ln(bpy)_2]Cl_3 \cdot 2H_2O$ complexes incorporated into the silica matrix strongly depended on the amount of complexes as incorporated and the temperature for the composite materials incorporated with 1 mol% of $[Ln(bpy)_2]Cl_3$ was evaluated to be about 300 °C for Ln = Tb and 450 °C for Ln = Eu. This indicated that the segregation of the complexes in the silica matrix tends to lower the temperature to start the decomposition of them. The silica matrix formed via the sol-gel route is porous, but the radius of pores is much smaller than the near-UV or visible radiation wavelength (1.5 - 10 nm)[27]. In addition, since the cage in the silica matrix containing lanthanide complex is probably even smaller than 1.5 nm, the matrix is consequently transparent[28]. As stated above, lanthanide complexes, $[Ln(bpy)_2]Cl_3 \cdot 2H_2O$ and $[Ln(phen)_2]Cl_3 \cdot 2H_2O$, are perhaps completely trapped in the rigid cages or bottleneck pores[29] separated with channels of the diameter smaller than the effective ones of ethanol or water[30]. In the case of $SiO_2$:$[Ln(bpy)_2]^{3+}$ (1 mol%), there exists individually each $[Ln(bpy)_2]Cl_3 \cdot 2H_2O$ complex in such cage of silica gel matrix for the incorporation with the complex below 1 mol% and hence the heat-resistance temperature increases to ca. 300 °C for $SiO_2$:$[Tb(bpy)_2]^{3+}$ and ca. 450 °C for $SiO_2$:$[Eu(bpy)_2]^{3+}$. However, the $[Ln(bpy)_2]Cl_3 \cdot 2H_2O$ complex was segregated in the rigid cage

with increasing its amount for the incorporation, and the heat-resistant temperature was gradually decreased.

The relative emission intensity of $SiO_2$:$[Tb(phen)_2]^{3+}$ (1 mol%) composite material was maximized at 300 °C, but the value was only 7 % (see Figure 1.14) and much lower than that of $SiO_2$:$[Tb(bpy)_2]^{3+}$ (1 mol%). This may be caused that the excited level of phen ligand was lower than that of bpy ligand and, in the course of the energy transfer from the phen ligand to $Tb^{3+}$ ion, the energy for excitation may return to the phen ligand. Therefore, it is apparent that the $[Tb(phen)_2]Cl_3 \cdot 2H_2O$ complex and $SiO_2$:$[Tb(phen)_2]^{3+}$ composite materials cannot emitted effectively rather than $[Tb(bpy)_2]Cl_3 \cdot 2H_2O$ complex and its composite materials.

## 1.5. Conclusion

A series of silica-based composite materials incorporated with lanthanide bipyridyl (bpy) and phenanthroline (phen) complexes, $SiO_2$:$[Ln(bpy)_2]^{3+}$ and $SiO_2$:$[Ln(phen)_2]^{3+}$ (Ln = Eu, Tb), were prepared by sol-gel method and their luminescence properties were studied before and after heat treatments up to 600°C. For the $SiO_2$:$[Ln(bpy)_2]^{3+}$ and $SiO_2$:$[Ln(phen)_2]^{3+}$ composites heated at appropriate temperatures, the energy transfer from the bpy or phen ligands to $Ln^{3+}$ ions smoothly took place as well as that for the original complexes and consequently the strong red or green emissions based on $Eu^{3+}$ and $Tb^{3+}$ ions were observed.

Emission outputs from the lanthanide complexes incorporated into silica gel matrice were intensified by optimizing the concentration of complexes and heating at individual temperature for heat treatment and the maxima of relative emission intensity (vs. $Y(P,V)O_4$:Eu and $LaPO_4$:Ce,Tb phosphors as practical used) were ca. 15 % and 45 % for $SiO_2$:$[Eu(phen)_2]^{3+}$ and $SiO_2$:$[Tb(bpy)_2]^{3+}$ composite materials. Furthermore, thermal stability of $[Ln(bpy)_2]^{3+}$ complexes was effectively improved compared with the original lanthanide complexes by incorporation into $SiO_2$ matrix.

# Chapter 2

## Luminescence Properties of Lanthanide Complexes into Sol-gel Derived Organic-inorganic Hybrid Materials

### 2.1. Introduction

In the previous Chapter, the luminescence characteristics of the europium and terbium complexes before and after incorporation into silica gel matrices by sol-gel method were studied. Although the composite materials with $[Eu(phen)_2]Cl_3 \cdot 2H_2O$ and $[Tb(bpy)_2]Cl_3 \cdot 2H_2O$ prosvide the red and green emissions with high colorimetric purity and furthermore the thermal stability and mechanical strength of the complexes were improved by silica gel matrix, their relative emission intensities were low compared with those of the original complex themselves because of the dilution of the complex concentration with the silica gel matrix. There exists a concentration limitation for incorporating the complexes (< several wt%), if the gel solutions containing large amounts of the complexes completely take place, the resulting composites become brittle and the transparency is lowered because of formation of crashes and segregation of the complexes.

On the other hand, silica-based hybrid matrices with three-dimensional skeleton structures of silica as silica units partially combine with oligomeric organosilane monomer unit, that is, organically modified silicates (ORMOSIL), have been prepared and their physical characteristics have been studied particularly on the optical one[31-35]. ORMOSIL has many advantages which are absent in silica and plastics for processing and physical properties as described in General Introduction.

In this Chapter, the ORMOSIL matrices containing methyl, phenyl, or propylmethacrylate groups as an organic component are incorporated with the lanthanide complexes, $[Eu(phen)_2]Cl_3 \cdot 2H_2O$ and $[Tb(bpy)_2]Cl_3 \cdot 2H_2O$ by the sol-gel method and their luminescence

properties are characterized on the basis of the measurements for luminescent spectra, thermal and hydration stability.

## 2.2. Experimental Section

Organic lanthanide complexes, $[Tb(bpy)_2]Cl_3 \cdot 2H_2O$ and $[Eu(phen)_2]Cl_3 \cdot 2H_2O$, were prepared according to the procedure described in Chapter 1. Appropriate amount of respective lanthanide complexes dissolved in N,N-Dimethylformamide (DMF, 99.9%, Wako Pure Chemical) was added in a mixed solution of water, ethanol (99.9%, Wako Pure Chemical), Tetraethoxysilane (TEOS, 99.9%, Wako Pure Chemical), and an organosiloxane such as diethoxydiethylsilane (DEDMS, 99.9%, Shin-Etsu Chemical Co., Inc.), diethoxydiphenylsilane (DEDPS, 99.7%, Shin-Etsu Chemical) or 3-(trimethoxysilyl)propyl methacrylate (TMSPM, 99.9%, Aldrich Chemical Co., Ltd.) with molar ratio of 11 : 7 : 3 : 1 by reflux thoroughly for 1 h. Dilute hydrochloric acid (0.005 M) was added tosol solution as a catalyst. The gel solutions obtained were cured at 50 °C over 10 days. The solidified ORMOSIL composite materials were then heated at 100 ~ 350 °C for 5 h in air. The excitation and emission spectra, IR spectra and relative emission intensities for these ORMOSIL composite materials were measured by the method in detail described in the previous Chapter.

## 2.3. Results

### *2.3.1. General results*

TMSPM, DEDMS and DEDPS were used as the oligomers because the organosilicates derived from them have the similar backbone structures, -Si-O-, to that of the silica matrix obtained from TEOS by the sol-gel method, and the plasticity owing to the intramolecular organic groups were improved compared with that of the conventional silica one. The inorganic and organic network modifiers used in this Chapter are shown in Figure 2.1. The organic network former, TMSPM (see Figure 2.1(b)), are usually connected to the silicon by Si-C bond, and the part of

(a) Inorganic network former

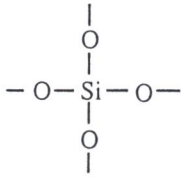

(b) Organic network former

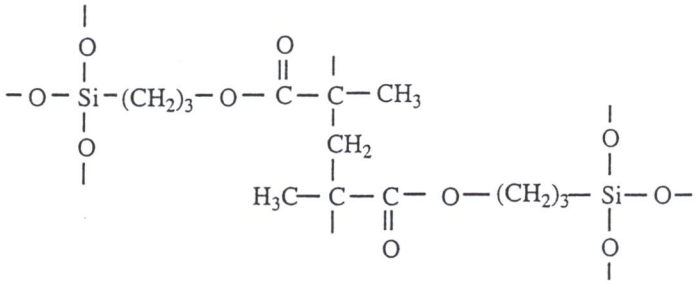

(c) Organic network modifiers

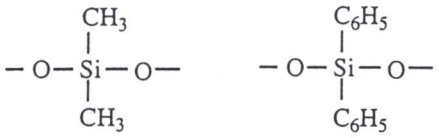

**Figure 2.1.** Network former and modifier units in ORMOSIL matrices.

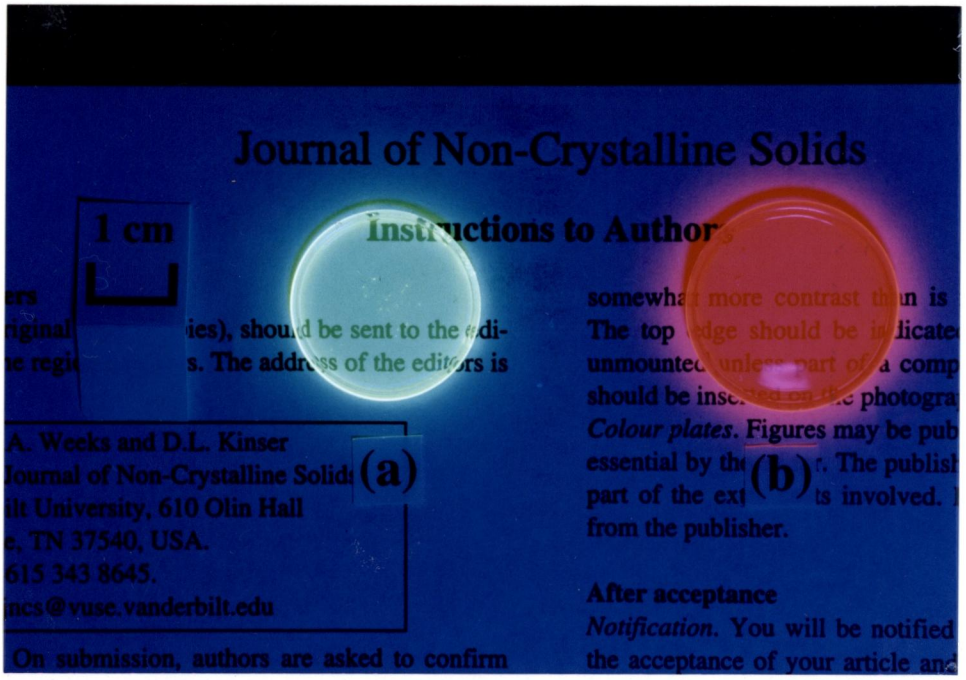


**Figure 2.2.** Photograph of the $SiO_2$/SPM:$[Tb(bpy)_2]^{3+}$ and $SiO_2$/SPM:$[Eu(phen)_2]^{3+}$ composite materials incorporated with 10 mol% of (a) $[Tb(bpy)_2]Cl_3$ and (b) $[Eu(phen)_2]Cl_3$ after aging and drying at 50˚C for more than two weeks.

-$Si(OH)_3$ derived from -$Si(OCH_3)_3$ in the molecular can condensate with TEOS and a propyl methacrylate groups in TMSPM can polymerize with one another. On the other hand, the organic network modifiers, DEDMS and DEDPS (see Figure 2.1(c)), have the parts of Si-methyl and Si-phenyl which cannot polymerize with other groups. Only the -$Si(OH)_2$ unit derived from -$Si(OC_2H_5)_2$ in DEDMS or DEDPS can condensate with TEOS[18]. In this Chapter, the author defines ORMOSIL matrix derived from DEDMS and TEOS as $SiO_2/Si(CH_3)_2O$, from DEDPS and TEOS as $SiO_2/Si(C_6H_5)_2O$, and from TMSPM and TEOS as $SiO_2$/SPM.

Figure 2.2 shows a typical photograph of $SiO_2/Si(CH_3)_2O$ composite materials doped with 10 mol% of the lanthanide complexes ($SiO_2/Si(CH_3)_2O$:$[Tb(bpy)_2]^{3+}$ (10 mol%) and $SiO_2/Si(CH_3)_2O$:$[Eu(phen)_2]^{3+}$ (10 mol%)) irradiated by a blacklight (UV excitation) from upper direction. Both the samples produced were transparent and free from cracks, and the strong red and green emissions were observed on the sample bulks, respectively. Although the matrices might somewhat become brittle, this was dependent upon the amount of oligomeric organosilicate component and the flexibility is improved by increase the contents. Therefore, the lanthanide complex should be incorporated into the ORMOSIL matrix compared with the TEOS only.

Typical IR spectra of lanthanide complex, $[Tb(bpy)_2]Cl_3$, and its composite materials, $SiO_2$/SPM:$[Tb(bpy)_2]^{3+}$ (1 - 20 mol%), heated at 150 °C for 5 h in air are shown in Figure 2.3. The composite materials provided typical absorption peaks in the regions of A (C=C and C=N stretch) and B (C-H out of plane bend) of which the intensities were enhanced with increasing the concentration of $[Tb(bpy)_2]Cl_3 \cdot 2H_2O$, apart from a strong absorption band based on the Si-O stretch in a wavenumber region of C, although they were superimposed on the original pattern of ORMOSIL. In addition, for the ORMOSIL:$[Tb(bpy)_2]^{3+}$ composite materials containing the excess amount of the complex (>10 mol%), the original absorption band of the $[Tb(bpy)_2]Cl_3$ complex as observed in the wave number region of C became significant and dominated the original absorption band based on the Si-O stretching of the ORMOSIL matrix. This indicates that the $[Tb(bpy)_2]Cl_3 \cdot 2H_2O$ complex is incorporated into the ORMOSIL matrix without any decomposition or serious modification. The absorption peak at 1670 $cm^{-1}$, especially suggested in Figure 2.4, was assigned to the C=C stretching mode for propylmethacrylate groups of TMSPM, indicating that the acrylate

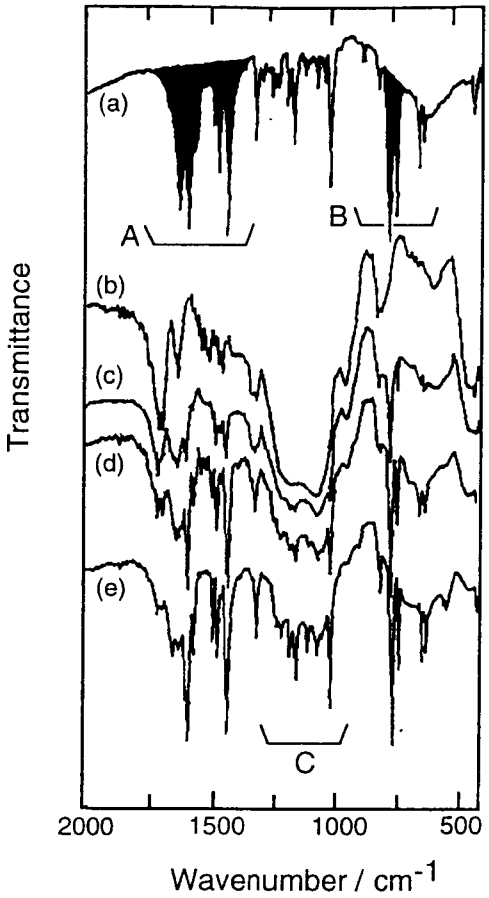


**Figure 2.3.** Typical IR spectra of (a) lanthanide complex ($[Tb(bpy)_2]Cl_3$) itself and (b-e) lanthanide complex doped ORMOSIL composite materials, $SiO_2$/SPM:$[Tb(bpy)_2]^{3+}$ (x mol%), with variousconcentrations of $[Tb(bpy)_2]^{3+}$: (b), x = 1; (c), x = 3; (d), x = 10; (e), x = 20. The composite materials were treated at 150°C for 5 h in air.

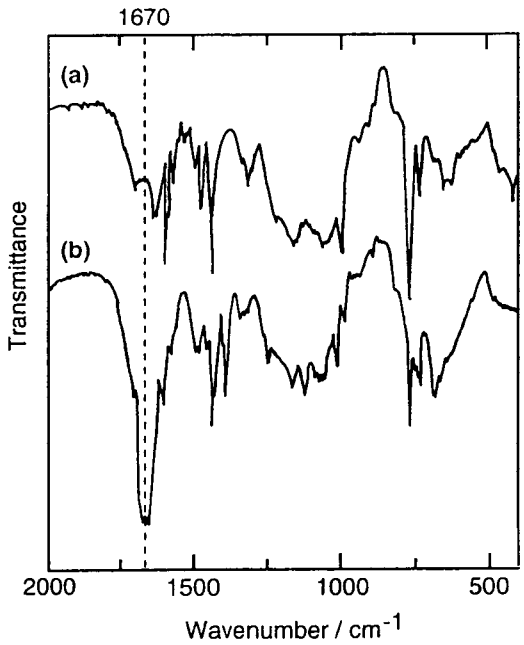


**Figure 2.4.** IR spectra of $SiO_2$/SPM:$[Tb(bpy)_2]^{3+}$ (10 mol%): (a) after heat treatment at 150°C for 5h and (b) without any heat treatment.

groups still remained in the ORMOSIL matrice without polymerization. However, such absorption signal almost disappeared by heating at the temperature above 150 °C. IR data for ORMOSIL matrices incorporated with $[Eu(phen)_2]Cl_3$ were the same result as described above.

### *2.3.2. Europium complex composite materials*

Excitation and emission spectra of $SiO_2$/SPM:$[Eu(phen)_2]^{3+}$ (10 mol%) as heated at 50, 150 and 300 °C are shown in Figure 2.5. The emission profile measured was closely similar to the emission spectrum of the original $[Eu(phen)_2]Cl_3 \cdot 2H_2O$ complex itself[16]: The red emissions were observed even on the composite materials incorporated with large amount of $[Eu(phen)_2]Cl_3 \cdot 2H_2O$ and were assigned to the $[Eu(phen)_2]^{3+}$ complex cation (see Figure 2.5a and 2.5b). On the other hand, two absorption bands existed in excitation spectrum profile, one at ca. 280 nm and another ca. 300 nm which were caused by the $SiO_2$/SPM matrix and the lanthanide complex, respectively. The excitation band as ascribed to ORMOSIL matrix was decreased with elevating the temperature for heat treatment. Therefore, the heat-resistance temperature of the ORMOSIL matrix was lower than that of the $SiO_2$ gel matrix prepared by sol-gel method. Particularly, the fact that the absorption band at around 310 - 340 nm based on the $\pi$ - $\pi^*$ band of phen ligands also reflects to the excitation spectrum pattern indicates that the $[Eu(phen)_2]^{3+}$ complex cations exist in the $SiO_2$/SPM matrix and they maintain the original molecular composition and structure. However, the excitation spectrum based on the phen ligand at ca. 310 - 340 nm decreased by the heat treatment at 300 °C. Consequently, the emission spectra of the ORMOSIL composite materials were significantly weakened compared with that of the sample heated up to 450 °C and only weak emission lines ascribed to the free $Eu^{3+}$ ion derived via decomposition of the complex was observed (see Figure 2.5c).

Heat treatment temperature dependencies of the relative emission intensity for $SiO_2$/SPM:$[Eu(phen)_2]^{3+}$ composite materials with various concentrations of the europium complex are shown in Figure 2.6. The relative emission intensity of the $SiO_2$/SPM:$[Eu(phen)_2]^{3+}$ composite materials were higher than that of the $SiO_2$:$[Eu(phen)_2]^{3+}$ with the corresponding

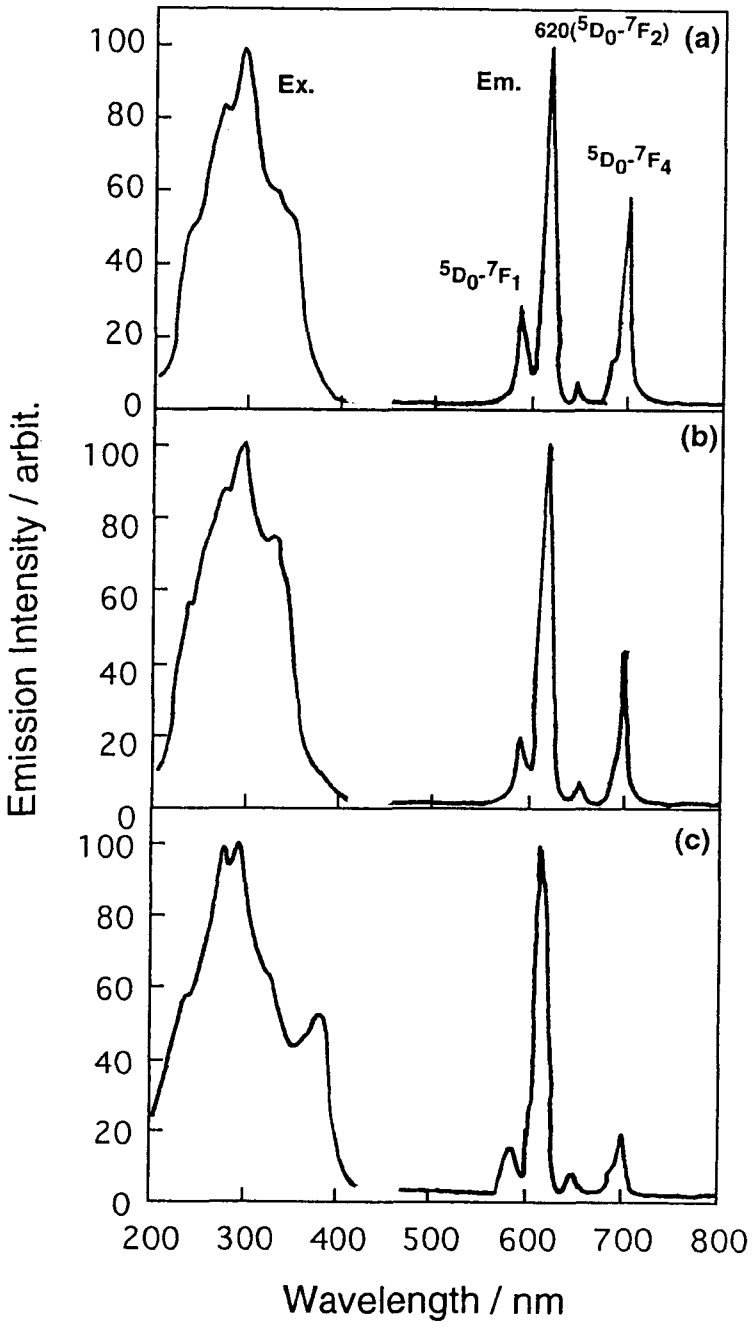


**Figure 2.5.** Excitation and emission spectra of the $SiO_2$/SPM:$[Eu(phen)_2]^{3+}$ (10 mol%) composite materials heated at various temperatures for 5 h in air : (a), 50°C; (b), 150°C; (c), 300°C.

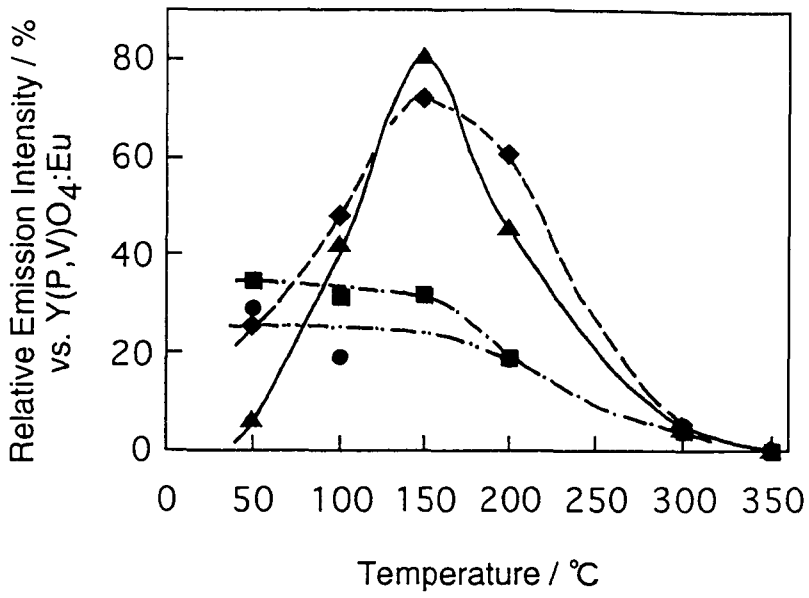


**Figure 2.6.** Heat-temperature dependencies of the relative emission intensity for $SiO_2$/SPM:$[Eu(phen)_2]^{3+}$ (x mol%) with concentration values of $[Eu(phen)_2]^{3+}$: (●), x = 1; (■), x = 3; (▲), x = 10 and (◆), x = 20. Heat treatments: in air, 5 h.

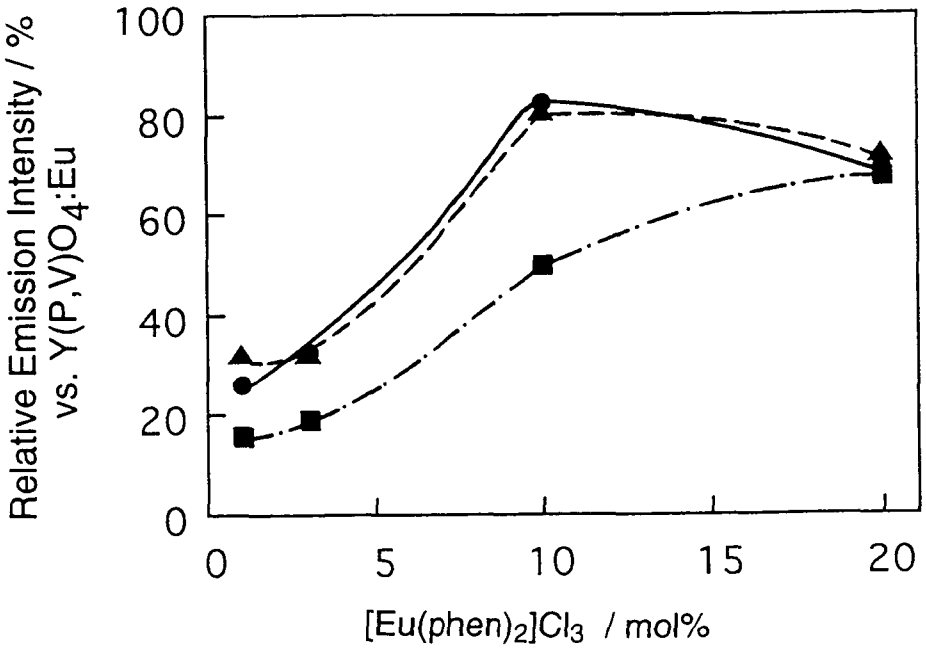


**Figure 2.7.** Complex-concentration dependencies of the relative emission inteisity for theORMOSIL:$[Eu(phen)_2]^{3+}$ composite materials obtained from various matrices: (●), ORMOSIL = $SiO_2$/SPM; (▲), $SiO_2/Si(C_6H_5)_2O$ and (■), $SiO_2/Si(CH_3)_2O$. Heat treatments: at 150°C in air, 5 h.

incorporation amounts of complexes. In the low temperature region below 150°C, the emission intensity of ORMOSIL composite materials was increased with elevating temperature for heat treatments. This would be due to the removal of solvated water from both the complexes and silica matrix, and consequently the condensation among the remaining silanol groups took place much more. As shown in Figure 2.7, the emission intensity for each composite materials at 150 °C was maximized by incorporation with 10 mol% of $[Eu(phen)_2]Cl_3$, providing a relative intensity value of about 80 %. It is noted that the specific intensity value per complex formula unit for the $SiO_2$/SPM:$[Eu(phen)_2]^{3+}$ is several times higher than that of the original $[Eu(phen)_2]Cl_3 \cdot 2H_2O$ complex and $SiO_2$:$[Eu(phen)_2]^{3+}$. Particularly, since the lanthanide complex incorporated into the ORMOSIL matrix was effectively protected from the moisture by the surrounding ORMOSIL units shown in Figure 2.1(b) and (c), their luminescence property was very stable after the standing in air, and we will represent this evidence later. In this case, the relative intensity was maximized by the heat temperatures at the relative high temperature of 150 °C. Therefore, the resulting $SiO_2$:$[Eu(phen)_2]^{3+}$ composite materials incorporated with ~ 20 mol% of $[Eu(phen)_2]Cl_3 \cdot 2H_2O$ was concluded to possess a good thermal stability comparatively, but a heat-resistance temperature of the ORMOSIL composite materials was decreased than that of the original $[Eu(phen)_2]Cl_3 \cdot 2H_2O$ complex.

### *2.3.3. Terbium complex composite materials*

Excitation and emission spectra of the $SiO_2$/SPM:$[Tb(bpy)_2]^{3+}$ (10 mol%) composite material heated at 50, 150 and 300 °C are shown in Figure 2.8. The peak at about 310 nm as observed on the excitation spectra of the $SiO_2/Si(C_6H_5)_2O$:$[Tb(bpy)_2]^{3+}$ composite materials heated to 50 and 150 °C (see Figure 2.8a and 2.8b), assigned to the $\pi$ - $\pi^*$ transition of the bpy ligand, and peak at 270 nm on the excitation spectra assigned to the absorption of excitation energy to the ORMOSIL matrix. Therefore, it is concluded that the chelated $Tb^{3+}$ ions, that is, the $[Tb(bpy)_2]Cl_3$ complex still exist in the ORMOSIL matrix prepared via the sol-gel process and the same molecular structure as the

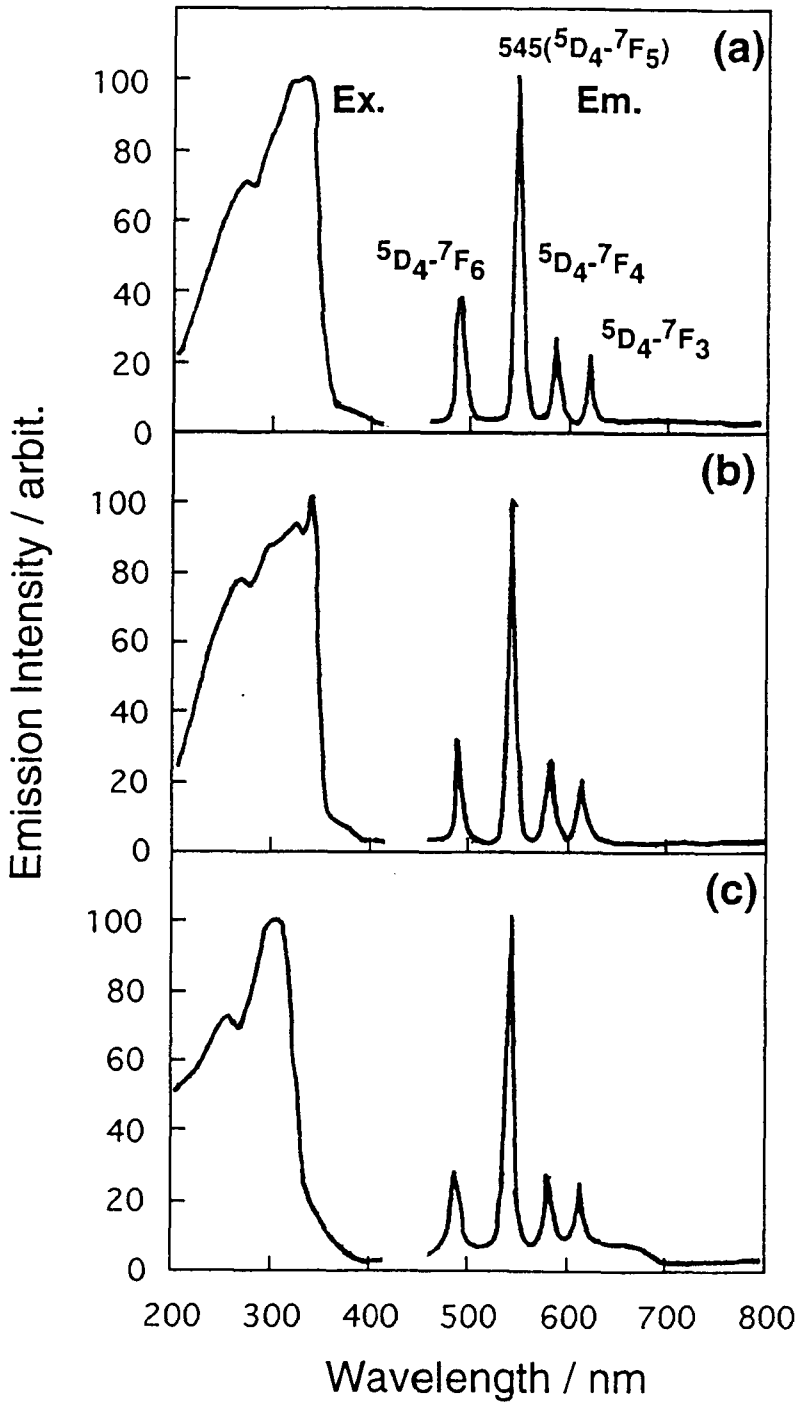


**Figure 2.8.** Excitation and emission spectra of the $SiO_2$/SPM:$[Tb(bpy)_2]^{3+}$ (1 mol%) composite materials heated for 5 h in air at various temperatures : (a), 50°C; (b), 150°C (c), 300°C.

original $[Tb(bpy)_2]Cl_3 \cdot 2H_2O$ complex was maintained even after heat treatment up to ca. 150 °C. However, the composite material heated to 300 °C provided a small band at about 310 nm on the excitation compared with the data heated to 50 and 150 °C. This means that the $Tb(bpy)_2^{3+}$ complex cation and/or ORMOSIL matrix are gradually decomposed over 150 °C. The emission spectrum pattern of $SiO_2/Si(CH_3)_2O$:$[Tb(bpy)_2]^{3+}$ composite materials consisted of four main lines at 489 nm ($^5D_4$ - $^7F_6$), 545 nm ($^5D_4$ - $^7F_5$), 586 nm ($^5D_4$ - $^7F_4$) and 622 nm ($^5D_4$ - $^7F_3$), and among them the emission lines at 545 nm was the strongest. The emission intensity of $SiO_2$/SPM:$[Tb(bpy)_2]^{3+}$ composite materials was extremely greater than those of $SiO_2$:$[Tb(bpy)_2]^{3+}$ . However, the emission intensity for the composite material heated to 300°C was decreased and there was no contribution to the energy transfer between the bpy ligand and the $Tb^{3+}$ ion.

The relationships between the treatment temperature and emission intensities for $SiO_2$/SPM:$[Tb(bpy)_2]^{3+}$ composite materials were shown in Figure 2.9. In the lower temperature region below 150°C, the emission intensity of terbium complexes was increased with temperature for the heat treatment by incorporating them to the $SiO_2$/SPM matrix. This is due to the dehydra-

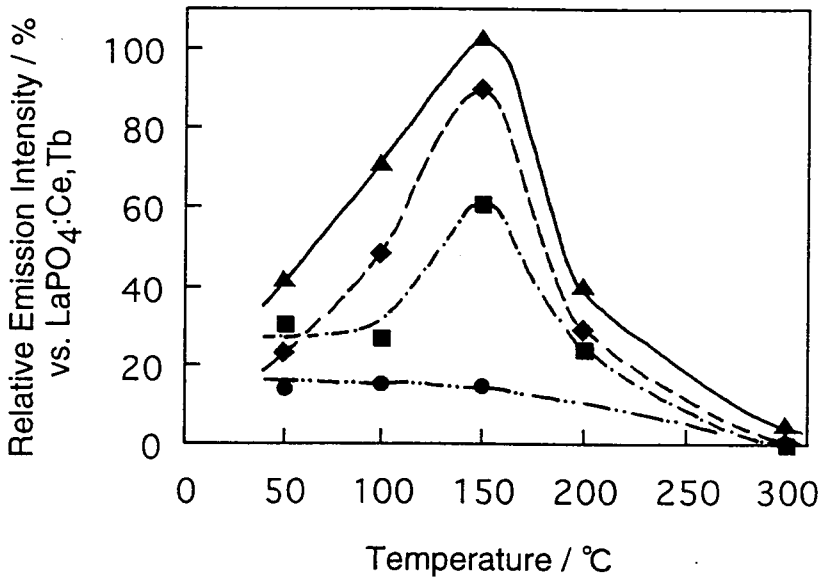


**Figure 2.9.** Temperature dependencies of the relative emission intensities for $SiO_2$/SPM:$[Tb(bpy)_2]^{3+}$ (x mol%) with various concentrations of $[Tb(bpy)_2]^{3+}$:(●), x = 1; (■), x = 3; (▲), x = 10 and (◆), x = 20. Heat treatments: in air, 5 h.

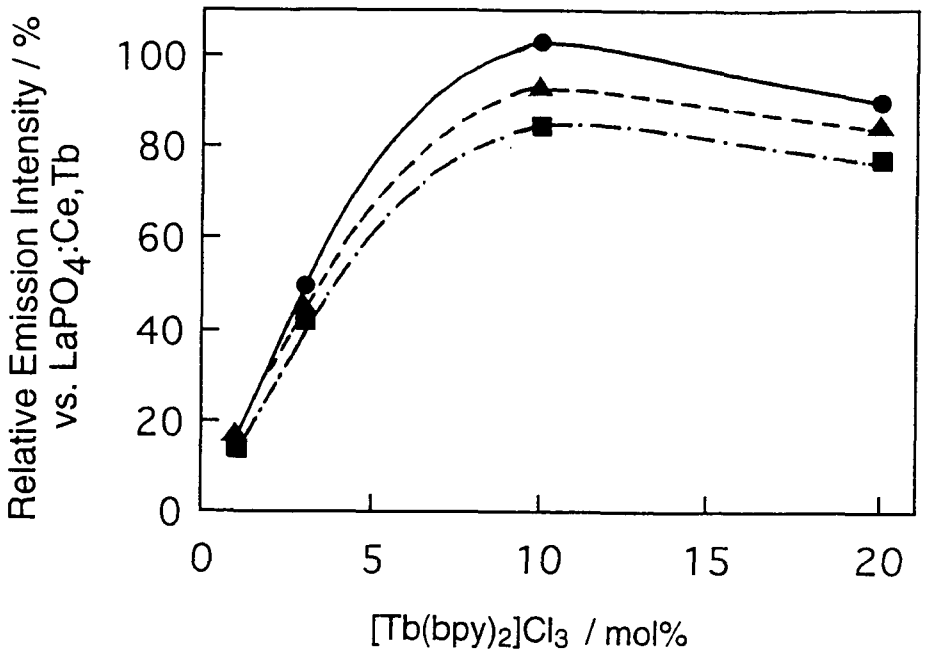


**Figure 2.10.** Complex-concentration dependencies of the relative emission inteisity for theORMOSIL:$[Tb(bpy)_2]^{3+}$ composite materials derived from various matrices: (●), ORMOSIL = $SiO_2$/SPM; (▲), $SiO_2/Si(C_6H_5)_2O$ and (■), $SiO_2/Si(CH_3)_2O$. Heat treatments: at 150°C in air, 5 h.

tion from both the complexes and ORMOSIL matrix, which contributes to depress the possibility of excitation energy loss *via* the multiphonon non-radiative process by water molecules. This effect could be explained by the fact that the multiphonon relaxation is due to the hydrated water molecules. The emission intensity of $SiO_2$/SPM:$[Tb(bpy)_2]^{3+}$ (1 mol%) was almost constant up to 150°C because the ORMOSIL matrix had been completely polymerized without the heat treatment and the $[Tb(bpy)_2]Cl_3 \cdot 2H_2O$ complex was incorporated as fully dispersed in the ORMOSIL matrix. The ORMOSIL:$[Tb(bpy)_2]^{3+}$ composite materials (ORMOSIL = $SiO_2/Si(C_6H_5)_2O$, $SiO_2/Si(CH_3)_2O$, $SiO_2$/SPM) incorporated with the larger amount of the complex than 10 mol% provided the maximum values at the heat temperature of 150 °C as shown in Figure 2.10, indicating that the $[Tb(bpy)_2]Cl_3 \cdot 2H_2O$ was effectively dispersed and incorporated into cage of ORMOSIL matrix in a similar manner as ORMOSIL:$[Eu(phen)_2]^{3+}$ (ORMOSIL = $SiO_2$/SPM, $SiO_2/Si(C_6H_5)_2O$). Particularly, it was noted that the relative emission intensity value (103 %) of the $SiO_2$/SPM:$[Tb(bpy)_2]^{3+}$ (10 mol%) composite material is comparable to that of the conventional phosphor, $LaPO_4$:Ce,Tb,

as practically used for the lamp illumination. The behavior that the emission intensity is increased by the heat treatment at the appropriate temperature is same as those of the original $[Tb(bpy)_2]Cl_3 \cdot 2H_2O$ complex and the $SiO_2$:$[Tb(bpy)_2]^{3+}$ composite materials of single matrix and is due to the dehydration of complexes. In addition, the mechanical strength of lanthanide complexes were improved by incorporation into the ORMOSIL matrices which are flexible. However, the thermal stability of those matrices is lower than that of the silica matrix derived from TEOS only, and then the emission intensity was gradually decreased by the heat treatment above 150 °C.

### *2.3.4. Stability against moisture*

Relationships between the relative emission intensities of the ORMOSIL composite materials or lanthanide complexes themselves and the standing time in air are shown in Figure 2.11. From this result, the lanthanide complexes were found to be effectively surrounded by ORMOSIL matrices so that they were shielded from the moisture in air, although the emission

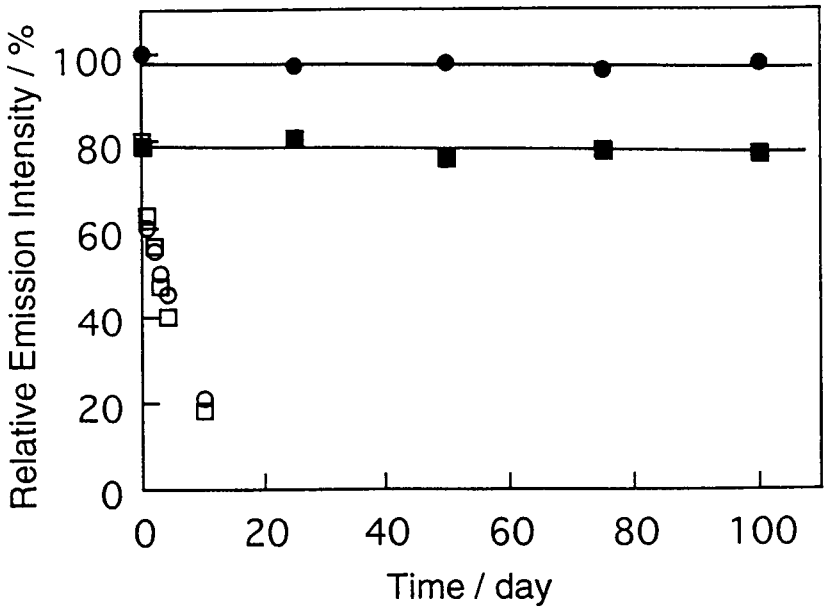


**Figure 2.11.** Relative emission intensities vs. standing time for: (●), $SiO_2$/SPM:$[Tb(bpy)_2]^{3+}$ (10 mol%);(■), $SiO_2$/SPM:$[Eu(phen)_2]^{3+}$ (10 mol%); (○), $[Tb(bpy)_2]Cl_3$ itself and (□), $[Eu(phen)_2]Cl_3$ itself. The standing was in air.

intensities of free lanthanide complexes were considerably decreased in several days. Therefore, one can concluded that the ORMOSIL composite materials incorporated with the lanthanide complexes possess the good stability enough to use practically as high-performance light-emitting materials with strong emission intensity and good transparency.

### *2.3.5. Lifetimes and Quantum yields*

Luminescence quantum yields and luminescence lifetimes for europium and terbium complexes and their ORMOSIL composites after heat treatment at 150 °C are summarized in Table 2.1 and 2.2, respectively.

Radiative and non-radiative rate constants are derived from the equation as follows:

$$\Phi = k\tau$$

$$1/\tau = k + k^*$$

where k and k* are the radiative and non-radiative rate constants, respectively. In these Tables, the radiative constant k is almost the same value of the order of $10^2$ and its value can be ascribed to the electric-dipole allowed, while k* value was $10^3$ $s^{-1}$.

**Table 2.1.** Luminescence properties of $Eu^{3+}$ complexes and their composite materials

| Sample | $\Phi^a$ / % | $\tau^b$ / μs | $k^c$ / $10^3 s^{-1}$ | $k^{*d}$ / $10^3 s^{-1}$ | $I^e$ / % |
|---|---|---|---|---|---|
| $[Eu(bpy)_2]Cl_3$ | 22.18 | 370.3 | 0.599 | 2.102 | 18.1 |
| $[Eu(phen)_2]Cl_3$ | 56.33 | 703.2 | 0.801 | 1.881 | 80.0 |
| $SiO_2$/SPM:$[Eu(phen)_2]^{3+}$ | 57.78 | 716.3 | 0.807 | 0,593 | 82.5 |
| $SiO_2/Si(C_6H_5)_2O$:$[Eu(phen)_2]^{3+}$ | 55.30 | 694.7 | 0.796 | 0.643 | 80.5 |
| $SiO_2/Si(CH_3)_2O$:$[Eu(phen)_2]^{3+}$ | 37.61 | 569.0 | 0.631 | 1.126 | 49.8 |
| $SiO_2$:$[Eu(phen)_2]^{3+}$ | 13.53 | 237.0 | 0.571 | 3.648 | 14.8 |

[a]Luminescence quantum yield. [b]Luminescence lifetime. [c]Radiative rate constant.
[d]Non-radiative rate constant. [e] Relative emission intensity vs. $Y(P,V)O_4$:Eu

**Table 2.2.** Luminescence properties of $Tb^{3+}$ complexes and their composite materials

| Sample | $\Phi^a$ / % | $\tau^b$ / μs | $k^c$ / $10^3 s^{-1}$ | $k^{*d}$ / $10^3 s^{-1}$ | $I^e$ / % |
|---|---|---|---|---|---|
| $[Tb(bpy)_2]Cl_3$ | 69.80 | 795.7 | 0.852 | 0.405 | 118.6 |
| $[Tb(phen)_2]Cl_3$ | 21.33 | 418.2 | 0.510 | 1.881 | 15.1 |
| $SiO_2$/SPM:$[Tb(bpy)_2]^{3+}$ | 67.78 | 816.3 | 0.855 | 0.373 | 103.0 |
| $SiO_2$/$Si(C_6H_5)_2O$:$[Tb(bpy)_2]^{3+}$ | 61.30 | 782.8 | 0.783 | 0.494 | 93.0 |
| $SiO_2$/$Si(CH_3)_2O$:$[Tb(bpy)_2]^{3+}$ | 56.61 | 754.8 | 0.750 | 0.575 | 85.0 |
| $SiO_2$:$[Tb(bpy)_2]^{3+}$ | 31.47 | 383.7 | 0.821 | 1.785 | 44.3 |

[a]Luminescence quantum yield. [b]Luminescence lifetime. [c]Radiative rate constant.
[d]Non-radiative rate constant. [e] Relative emission intensity vs. $LaPO_4$:Ce,Tb

## 2.4. Discussion

In the preparation process, as the ORMOSIL materials were prepared without refuxing the sol solution containing 0.005M HCl as a catalyst, took place the phase separation to inorganic and organic rich one. This would be due to the difference of the hydrolysis rate between TEOS and organosilane. However, no phase separation and cracking were observed on the resulting matrix with refluxing for 1 h. This is due that the condensation between the silanol groups in TEOS and organosilane precursors completely proceeds by refluxing.

The ORMOSIL composite materials incorporated with tha lanthanide matrices have been only succeeded in preparing in the homogeneous form as the photograph presented in Figire 2.2 as DMF solution of lanthanide complexes are added in the ORMOSIL sol solution. In the case of ethanol solutions or aqueous solutions of the lanthanide complex, any homogeneous product is not obtained because of the precipitation of the complex. This is caused by the fact that the vaporizing rate of the solvent for lanthanide complex is almost equal to the condensation rate of silanol in the ORMOSIL matrices since the boiling point of DMF is higher than those of EtOH and water. Furthermore, DMF is an aprotic solvent and has an affinity for organic compounds by its large polarity. Therefore, it is considered the lanthanide complexes are effectively dispersed and

embedded in the ORMOSIL matrices before precipitating the complex.

The lanthanide complexes which are properly incorporated into the sol-gel derived ORMOSIL host materials are encapsulated by a 'cage' in those matrices. Especially, by heat treatments at the lower temperature (<150 °C), rigid cages are expected to be formed in the flexible three-dimensional network composed by copolymerization among silica and propylmethacrylate units which are strongly cross-linked and in which the complexes can be embedded[36]. Such silica-acrylate, silica-methyl and silica-phenyl cages around the $[Eu(phen)_2]Cl_3$ and $[Tb(bpy)_2]Cl_3$ are only constructed under the presence of acid and reflux conditions for the preparation process. Therefore, the previous result that the larger amount of lanthanide complexes cannot be well incorporated in the silica matrix is ascribed to the rigid framework of silica which provide no such flexible cage.

On the other hand, although the condensation reactions among the silanol groups have been reported to be accelerated by addition of a basic catalyst, the complexes are scarcely incorporated into the ORMOSIL matrices. Furthermore, the preliminary studies on the incorporation of the lanthanide complexes into titania-silicate gels provide some results that the interactions of these complexes into the titania-silicate matrix as expected to form do not occur but preferentially take pkace into titania particles because only titania component has condensated[37]. These results indicate that the initial stage for the cage construction takes place around the lanthanide complexes as templates at the sol formation step of the sol-gel process. The interactions between complexes and ORMOSIL matrix probably exist even in the 'sol phase' (solution) before prolonged condensation proceed, as shown by the unsuccessful incorporation under basic conditions. However, at this stage the incorporation of the complexes is not completed. The final stage of the cage construction is during the drying process of the matrix, , resulting in complete encapsulation of the lanthanide complexes,[38-40].

Heat-resistance temperature of lanthanide complexes incorporated into the ORMOSIL matrices were evaluated to be about 150°C for $SiO_2$/SPM:$[Tb(bpy)_2]^{3+}$ and 150 - 200 °C for $SiO_2$/SPM:$[Eu(phen)_2]^{3+}$ and did not depend on the amount of complexes even though much more amount of complexes than the case of the silica gel composite materials derived from TEOS only

incorporated into the ORMOSIL matrices. The ORMOSIL matrix formed *via* the sol-gel route are flexible compared with the silica gel prepared by the same way, and furthermore the radius of such pore is much smaller than that of sol-gel silica matrix. In addition, since the cage in the ORMOSIL matrix containing lanthanide complex is probably even less than 1.5 nm and thelanthanide complexes are effectively dispersed in the ORMOSIL matrices, the composite materials are consequently transparent [39,39]. As stated above, lanthanide complexes, $[Tb(bpy)_2]Cl_3 \cdot 2H_2O$ and $[Eu(phen)_2]Cl_3 \cdot 2H_2O$, are perhaps completely introduced in the larger cages formed by the organic group such as $CH_3$, $C_6H_5$, and propylmethacrylate in ORMOSIL, and effectively stabilized from the moisture in air.

The behavior that the red and green emissions are intensified by heat treatments are due to the elimination of the solvated water which plays a role as a inhibitor for the energy transfer from the excited ligands to the lanthanide ions in the matrix, and also such elimination enhances the further polymerization among the organosilane and TEOS residues by which the complexes are fully incorporated and homogeneously dispersed in these matrix. These results are supported by the IR spectrum data shown in Figure 2.3 and described in Chapter 1. The reason why the relative emission intensity of the composite materials containing the excess amount of the complexes, *e.g.* $SiO_2$/SPM:$[Tb(bpy)_2]^{3+}$ (20 mol%) and $SiO_2$/SPM:$[Eu(phen)_2]^{3+}$ (20 mol%), was decreased rather than the composite one incorporated with the smaller amount (10 mol%) of lanthanide complexes might be due to a concentration quenching. The lanthanide complexes tend to segregated in the cracks and grain boundaries induced in the ORMOSIL matrix with increasing the amount of the complexes. Therefore, it is concluded that the amount up to 10 mol% of the lanthanide complexes can be a stably incorporated into the ORMOSIL matrices.

For the resulting the luminescence characteristics of lanthanide complexes and their composite materials, the enhancement of the emission intensity is owing to a decrease in the k* value (see Tables 1 and 2). However, the lanthanide complexes, for example, $[Eu(bpy)_2]Cl_3$ and $[Tb(phen)_2]Cl_3$,exhibited the lower emission intensity where the k* values were larger. The excited $Eu^{3+}$ ion is non-radiatively deactivated by transfering the excited energy from $Ln^{3+}$ to ligands and the decrease of asymmetry of $Eu^{3+}$ ion in the complex. The magnitude of k* will, therefore, be

strongly dependent on the energy level between ligand and $^5D$ transition level of the lanthanide ion, and the symmetry of the complexes. As its number of water molecules decreases around lanthanide ion chelated organic ligands, the value of k* decreases and the luminescence quantum yield becomes larger. It is shown that the energy transfer is very effective and the lifetimes of the excited ($^5D_0$) europium is long enough to provide good luminescence intensity. The lifetime of the phen complex is longer than that observed in bpy complex, which is cited as a strong luminescent system. In particular, the $^5D_0$-$^7F_2$ transition in the $[Eu(phen)_2]Cl_3$ complex and its ORMOSIL composites is approximately five times more intense than the $^5D_0$-$^7F_1$ transition of them, and the $^5D_0$-$^7F_4$ transition also is considerable intensified. The luminescence spectrum of the complex suggests that the $Eu^{3+}$ site symmetry is preserved. It is similar to the spectra obtained from the inorganic solid compounds using a conventional lump phosphor.

The analogous terbium(III) complexes have also been synthesized and characterized. The strong emission intensity for $[Tb(bpy)_2]Cl_3$ and its ORMOSIL composite materials would be most likely due to a large energy gap between the bpy triplet level and the $^5D_4$ level of $Tb^{3+}$ ion. On the other hand, the emission intensity of $[Tb(phen)_2]Cl_3$ was considerably weakened rather than that of $[Tb(bpy)_2]Cl_3$. This would be due to the reversible energy transfer from $Tb^{3+}$ ion to phen ligand because the energy gap between them is smaller than that of $[Tb(bpy)_2]Cl_3$ complex.

## 2.5. Conclusion

Lanthanide complexes such as $[Tb(bpy)_2]Cl_3$ and $[Eu(phen)_2]Cl_3$ incorporated into the organically modified silicates (ORMOSIL) were prepared and their luminescence characteristics were investigated. The resulting products of these ORMOSIL composite materials were so clear, and could be increased in the incorporation amount of lanthanide complex up to 20 mol%.

The emission intensities for the ORMOSIL composite materials incorporated with 10mol% of $[Tb(bpy)_2]Cl_3$ and $[Eu(phen)_2]Cl_3$ after heat treatment at 150°C for 5 h in air were 100 and 80 % compared with that of the conventional lamp phosphors used as a standard, respectively.

In addition, the relative emission intensities of these composite materials incorporated with 10 mol% of the lanthanide complexes which were left in air were not changed more than 100 days. This is caused that the lanthanide complexes are effectively dispersed and surrounded by the ORMOSIL matrices and water molecules decreased around the complexes by heat treatment.

# Chapter 3

## Photovoltaic Cell Characteristics of Hybrid Silicon Devices with Lanthanide Complex Phosphor Coating Film

### 3.1. Introduction

In Chapter 2, the luminescence properties of organic lanthanide complexes, $[Eu(phen)_2]Cl_3$ and $[Tb(bpy)_2]Cl_3$, incorporated into ORMOSIL[41-45], were investigated. Their relative emission intensities were nearly found equal to conventional lamp phosphors.

Recently, the maximal outputs of the photovoltaic cells (PVC) have been attempted to be enhanced by their surface improvements [46-49] or using other semiconductors[50-53]. On the other hand, silicon solar cells are among the most promising materials for the energy conversion of sunlight to electric power, but, in the case of Si PVC, the light transformation efficiency in UV region is significantly lower than that in visible one. The spectroscopic sensitivity curve of amorphous silicon (a-Si) and single crystal silicon (c-Si) solar panels provides an absorption edge in the shorter wavelength region at about 300 nm, and furthermore, the light intensity in this region is much lowered by the additional absorption of the resin film coated practically for protection. Consequently, the sunlight fractions at the shorter wavelength are completely wasted in such PVC system. However, if the UV lights are converted to the visible ones which are sensitive for Si PVC by efficient photoluminescent materials, one can expect a considerable enhancement in the PVC conversion efficiency. Indeed, $[Tb(bpy)_2]Cl_3$ provides strong line emissions, and the main line of them peaks at 545 nm, which is very close to the peak of spectroscopic curve of a-Si (550 nm), and the strong emission line peaking at 620 nm is observed on $[Eu(phen)_2]Cl_3$, which closely meets the peak of spectroscopic curve of c-Si (700 nm)[54].

In the present Chapter, the silica-based ORMOSIL composite matrices, which have been demonstrated and characterized as suitable host materials for organic compounds, *e.g.* dyes and lanthanide complexes, were prepared by sol-gel method and incorporated with $[Eu(phen_2]Cl_3$ and $[Tb(bpy)_2]Cl_3$. Furthermore, the hybrid solar cell devices are fabricated by coating with the resulting ORMOSIL composite materials on the surface of c- and a-Si solar cell panels, and their conversion characteristics of sunlight to electric power were studied.

### 3.2. Experimental Details

The lanthanide complex and ORMOSIL matrices, which was defined in this study as $SiO_2$/SPM, used here have been prepared according to the procedure described in Chapter 2. The viscous gel solutions of ORMOSIL composite materials derived from TEOS and 3-(trimethoxysilyl)-propylmethacrylate containing various amounts of $[Tb(bpy)_2]Cl_3$ or $[Eu(phen)_2]Cl_3$ were coated on the surface of the commercially available a-Si PVC (TDK Co., Ltd.) which consisted of p-i-n structure of amorphous Si or c-Si PVC (SOLARTECH Co., Ltd.) panels which consisted of p-n structure of single crystal Si covered with polyester laminate film and dried at 50 °C for more than

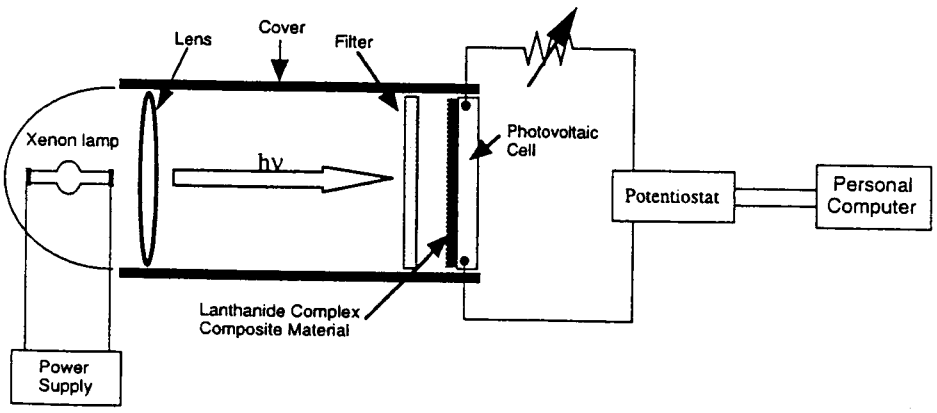


**Figure 3.1.** Apparatus for the measurement for V-I chacteristics Si PVC.

38 h in air, respectively. The excitation and emission spectra of the resulting lanthanide complexes incorporated into $SiO_2$/SPM matrix ($SiO_2$/SPM:$[Tb(bpy)_2]^{3+}$ and $SiO_2$/SPM:$[Eu(phen)_2]^{3+}$) were measured by the method described in Chapter 2. Measurements for the V-I characteristics of the a- and c-Si PVC hybrid devices were carried out on a solar simulator with xenon lamp (100 $mWcm^{-2}$) at room temperature and the UV lights below 300 nm were cut by a glass filter as illustrated in Figure 3.1. The enhancement in electric outputs of a- and c-Si PVC hybrid devices was evaluated in comparison with those of the non--coated a- and c-Si PVC.

## 3.3. Results and discussion

### *3.3.1. Characteristics of c-Si PVC with europium complex ORMOSIL coating film*

Excitation and emission spectra of the ORMOSIL composite material containing 3 mol% of $[Eu(phen)_2]Cl_3$ as dried at 50 °C are shown in Figure 3.2, together with the spectroscopic

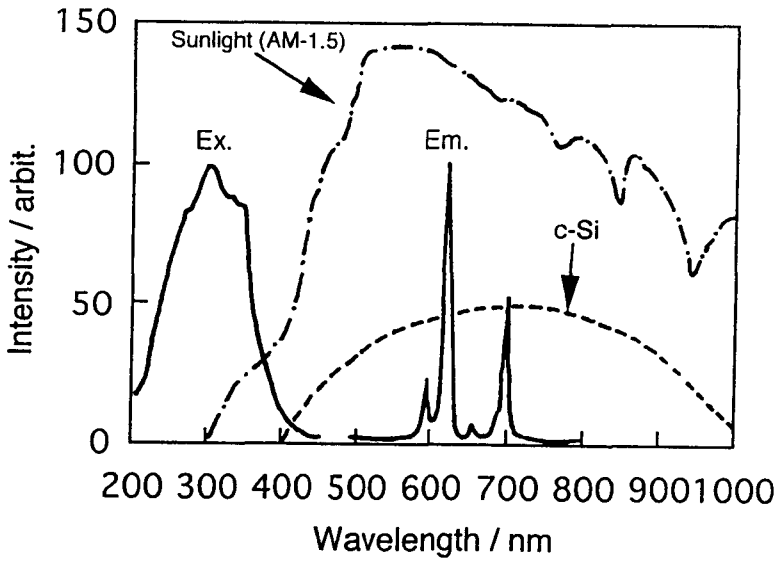


**Figure 3.2.** Typical excitation and emission spectra of ORMOSIL ($SiO_2$/SPM) composite materials doped with $[Eu(phen)_2]Cl_3$ (solid line). The dotted and dashed lines represent the usual sunlight spectrum and the spectroscopic sensitivity curve of c-Si solar cell, respectively.

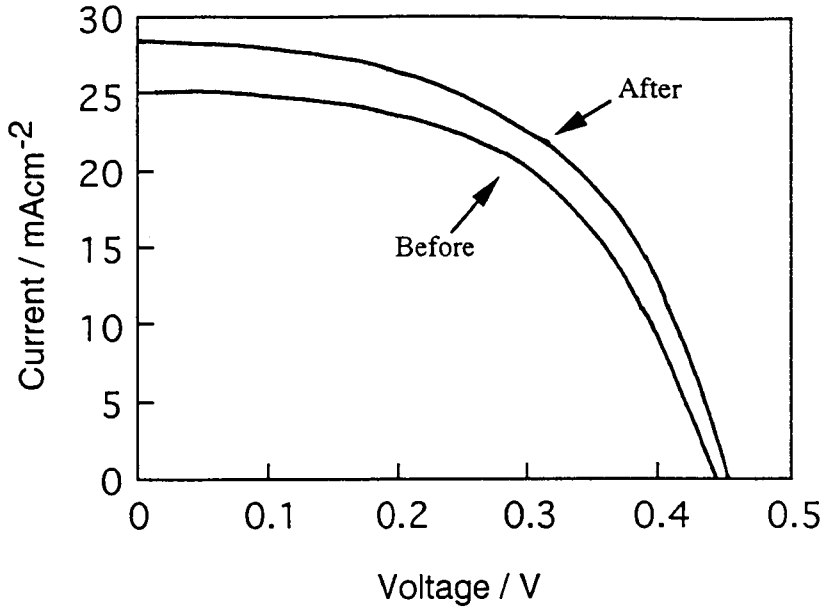


**Figure 3.3.** V-I characteristics of a c-Si PVC devices obtained under the same condition of modulated sunlight irradiation with the surface before and after coating with the $SiO_2$/SPM:$[Eu(phen)_2]^{3+}$ composite film (thickness = ca. 1.0 mm). The illuminated area was about 2.5 x 5.2 $cm^2$.

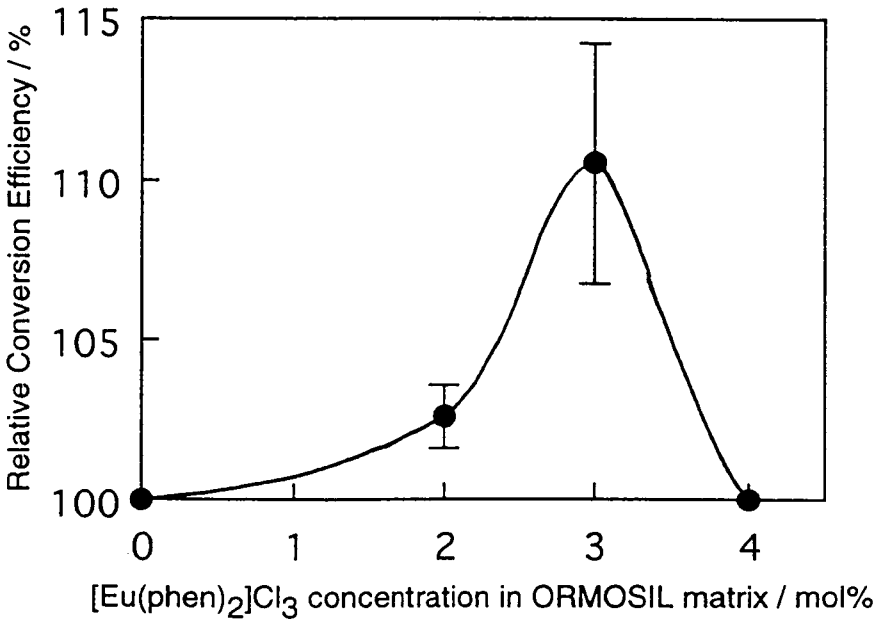


**Figure 3.4.** Complex concentration dependence of the relative conversion efficiency for the hybrid c-Si PVC devices with $SiO_2$/SPM:$[Eu(phen)_2]^{3+}$ composite film.

sensitivity curve of the commercial c-Si PVC and spectrum of sunlight (AM-1.5). The lanthanide complex composite material used strongly absorbs the light in the region from 310 to 340 nm and emits it at 620 nm. It is found that enhancement of outputs by this wavelength shifting using europium complex is possible in the relative long wavelength sensitivity of the PVC.

The ORMOSIL doped with $[Eu(phen)_2]Cl_3$ of 1 ~ 4 mol% was dripped onto the surface of the c-Si PVC resulting in an ~ 0.3 mm thick film after drying at temperature of 50 °C. According to this method of c-Si PVC coating, the outputs of the PVC were increased. The resulting V-I characteristics of the c-Si PVC hybrid devices coated with the ORMOSIL composite material film were shown in Figure 3.3, together with those of uncoated c-Si ones. The enhanced outputs for the coated c-Si PVC were obtained.

The concentration dependence of the europium complex on the relative conversion efficiency under the same irradiation condition is shown in Figure 3.4. The maximal outputs increase gave a value of 10% at $[Eu(phen)_2]Cl_3$ concentration of 3 mol% in ORMOSIL matrix. However, the outputs was decreased with increasing the amount of $[Eu(phen)_2]Cl_3$, and finally, the value of the outputs were lower than 100% at coating ORMOSIL composites doped over the amount of 5mol%.

### *3.3.2. Characteristics of a-Si PVC with terbium complex ORMOSIL coating film*

Excitation and emission spectra of the ORMOSIL composite material containing 2 mol% as dried at 50 °C are shown in Figure 3.5 for $[Tb(bpy)_2]Cl_3$, together with the absorption curve of the commercial a-Si PVC and spectrum of sunlight (AM-1.5). In this case, the excitation (absorption) spectrum of lanthanide complex gave a strong band peaking at ca. 310 nm, which was as attributed to the $\pi$ - $\pi^*$ transition of bpy ligands, followed by the intense line emissions in the visible region via the energy transfer from the ligands to $Tb^{3+}$ ions. However, the absorption spectrum pattern of $SiO_2$/SPM:$[Tb(bpy)_2]^{3+}$ was kept at the background level in the visible region sensive for the a-Si PVC. These results indicate that the $SiO_2$/SPM:$[Tb(bpy)_2]^{3+}$ composite material is suitable as a modulator to enhance the electric outputs of a-Si PVC because the sunlight fraction in the higher energy region as unsensitive for PVC is effectively converted to the useful visible

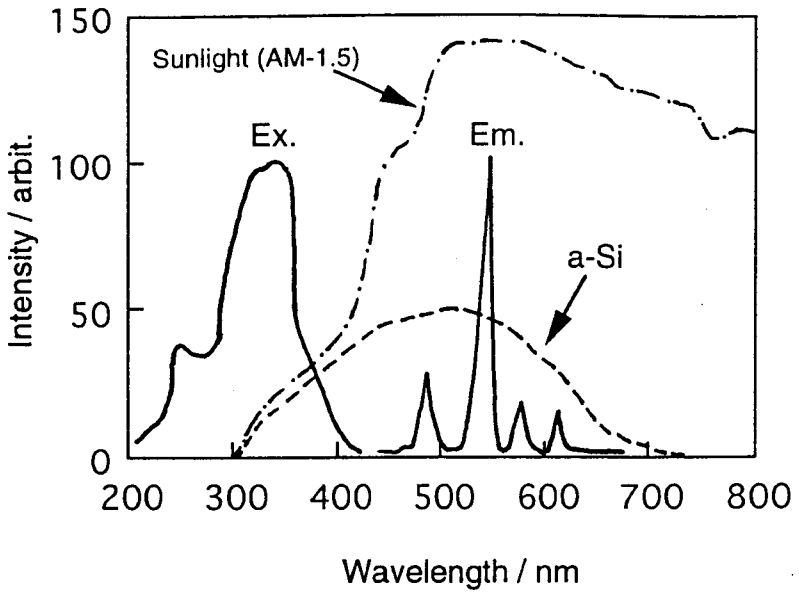


**Figure 3.5.** Typical excitation and emission spectra of ORMOSIL ($SiO_2$/SPM) composite material doped with $[Tb(bpy)_2]Cl_3$ (solid line). The dotted and dashed lines represent the usual sunlight spectrum and the spectroscopic sensitivity curve of a-Si solar cell.

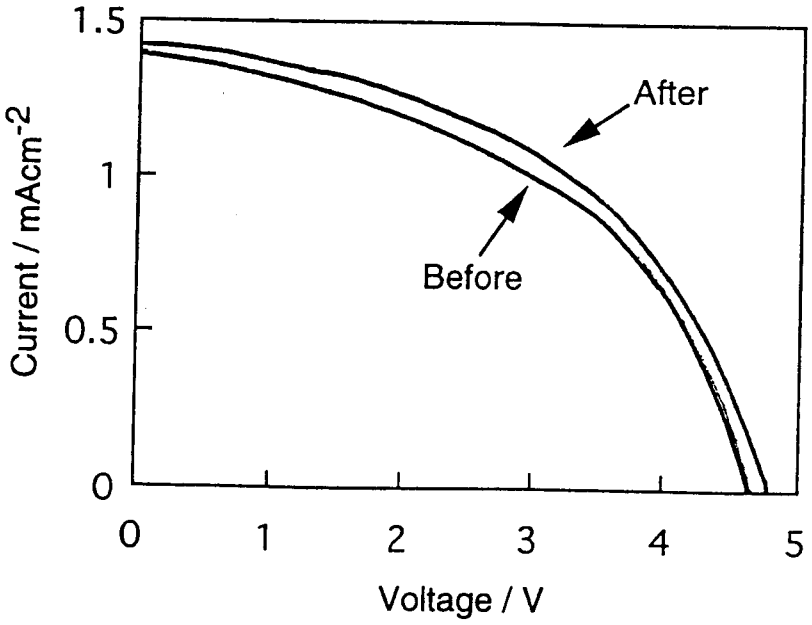


**Figure 3.6.** V-I characteristics of an a-Si PVC devices obtained under the same condition of modulated sunlight irradiation with the the surface before and after coating with the $SiO_2$/SPM:$[Tb(bpy)_2]^{3+}$ composite film (thickness = ca. 0.1 mm). The illuminated area was about 4.0 x 6.5 $cm^2$.

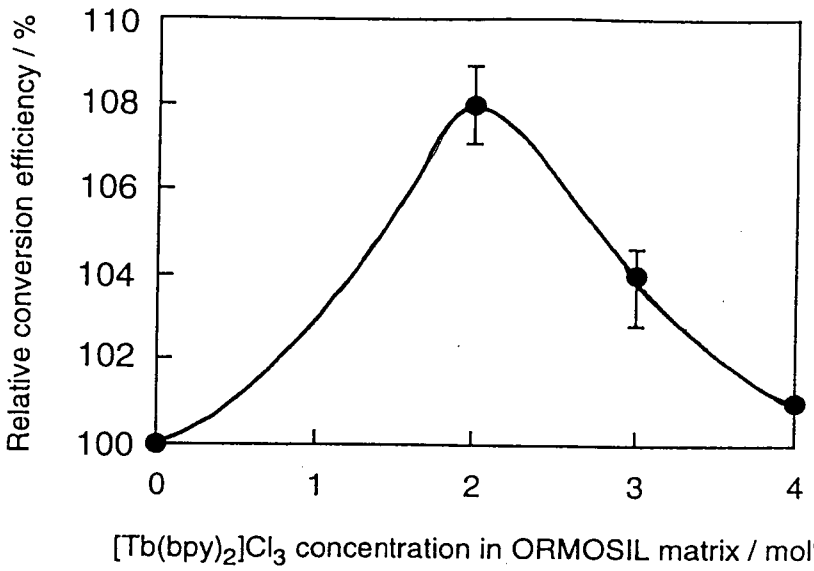


**Figure 3.7.** $[Tb(bpy)_2]Cl_3$ complex concentration dependence of the relative conversion efficiency for the a-Si PVC with the surface coating film of $SiO_2$/SPM:$[Tb(bpy)_2]^{3+}$ composite material.

lights by the terbium complex.

The V-I characteristics of the a-Si PVC hybrid devices coated with the $SiO_2$/SPM composite material film were measured, together with those of uncoated a-Si ones (see Figure 3.6). From the results, the relative conversion efficiency was increased to ca. 8 % by such coating. In addition, the concentration dependence of the terbium complex on the relative conversion efficiency under the same irradiation condition is shown in Figure 3.7. The efficiency was maximized at the dopant concentration of 2 mol%, of which the hybrid device provided the further enhancement around 8%.

### *3.3.3. The reflectivities of ORMOSIL composites coated PVC and non-coated PVC*

The reflectivity measured on the hybrid a-Si PVC was approximately ca. 7% higher than that of non-coated PVC in the region from 330 to 800 nm (see Figure 3.8). In practice, the preliminary experiments demonstrated that the maximal output might be enhanced to be 20 % higher than that of the respective uncoated Si PVC by optimizing the chemical

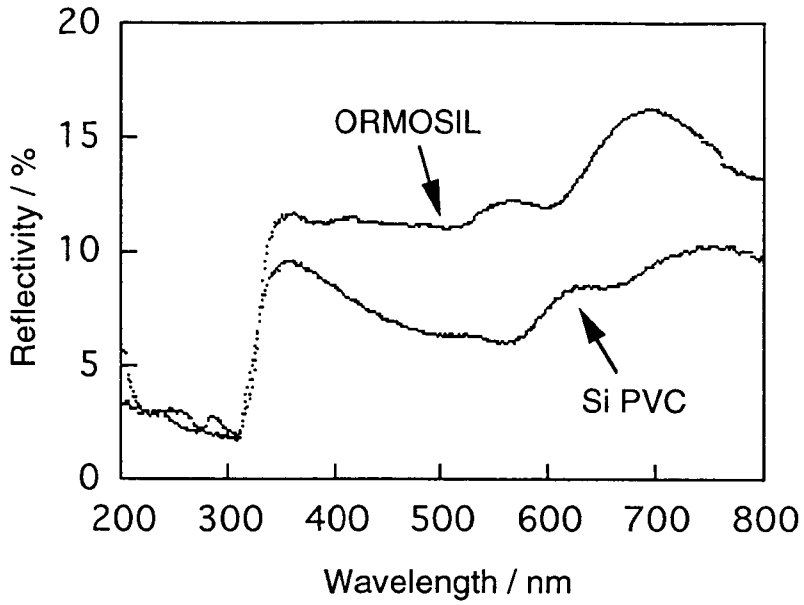


**Figure 3.8.** The reflectivity on the surface of ORMOSIL and Si PVC.

composition between the silica and organosilane. Also, the luminescence characteristics of ORMOSIL composite materials are strongly dependent on the coating conditions, the surface conditions, film thickness and subsequent heat treatment conditions. It is expected that the outputs for respective Si PVC enhance by coating ORMOSIL composite film after controlling the above factors.

### 3.5. Conclusion

Maximal outputs of amorphous silicon (a-Si) and single crystal silicon (c-Si) photovoltaic cells (PVC) coated by the organically modified silicate (ORMOSIL) composite film containing a terbium bipyridine complex were increased to be 8% for a-Si hybrid PVC device and 10 % for c-Si hybrid PVC device higher than those of the non-coated Si PVC. These are owing to the effective optical modulation from UV to visible light by the lanthanide complex incorporated into the ORMOSIL matrix.

# Summary

In this work of this thesis, luminescence characteristics of the europium (III) and terbium (III) complexes doped into silica-based glass matrices have been studied and discussed for the purpose to develop new red or green emitting photoluminescent devices.
The results deduced from this work are summarized as follows:

**Chapter 1.** The relative emission intensities of lanthanide complexes, *e.g.* $[Ln(bpy)_2]Cl_3 \cdot 2H_2O$ and $[Ln(phen)_2]Cl_3 \cdot 2H_2O$ (Ln = Eu and Tb), were considerably increased by heat treatments and maximized at the suitable temperatures. Particularly, $[Eu(phen)_2]Cl_3 \cdot 2H_2O$ and $[Tb(bpy)_2]Cl_3 \cdot 2H_2O$ gave the strong red and green emission with the relative emission intensities of 18 ~ 120 % versus the $Y(P,V)O_4$:Eu and $LaPO_4$:Ce,Tb standards phosphor as practically used by the heat treatment at 150 °C. However, the emission intensities of the resulting materials derived from the complexes were gradually decreased due to the moisture in air.

The lanthanide complexes were succeeded in incorporating into the $SiO_2$ matrix prepared by sol-gel method without any decomposition and serious change of them. Consequently, the thermal stability of these lanthanide complexes was effectively improved by incorporation into the silica matrix.

The emission spectra of lanthanide complexes were intensified by incorporating them into silica matrix, and their specific emission intensities per complex formula unit effectively increase compared with those of the original lanthanide complexes. The composite materials prepared under the optimized conditions provided the strong red or green emissions with the relative intensity value of 17 % for $SiO_2$:$[Eu(bpy)_2]^{3+}$ (1 mol%), 15 % for $SiO_2$:$[Eu(phen)_2]^{3+}$ (3 mol%), and 44 % for $SiO_2$:$[Tb(bpy)_2]^{3+}$ (10 mol%), respectively. Therefore, the relative intensities of the composite materials are expected to be intensified much more if the lanthanide complexes are highly dispersed in the matrices.

**Chapter 2.** The much larger amount of lanthanide complexes than into the above-mentioned silica matrix were incorporated into an ORMOSIL matrix than into a silica matrix by sol-gel process without any decomposition. Furthermore, the samples obtained were transparent and free from usual cracking problem, and the strong green and red luminescences were observed on the sample monoliths irradiated by UV light.

A systematic study on the luminescence properties of the lanthanide complexes, $[Eu(phen)_2]Cl_3$ and $[Tb(bpy)_2]Cl_3$, incorporated into some ORMOSIL matrices *via* the sol-gel process demonstrated that the resulting ORMOSIL composite materials prepared provide the strong green and red emission, of which their relative emission intensities were improved to be approximately equal to those of the conventional lamp phosphors such as $Y(P,V)O_4$:Eu and $LaPO_4$:Ce,Tb by optimization of the preparation conditions.

**Chapter 3.** The maximal outputs of the commercial amorphous (a-Si) and single crystalline silicon (c-Si) photovoltaic cells (PVC) were effectively enhanced by simple coating of the ORMOSIL composite materials incorporated with the terbium and europium complexes which can convert the UV light to the visible ones as photoemissions.

The conversion efficiencies for each PVC were strongly dependent on the coating film conditions of $SiO_2$/SPM:$[Tb(bpy)_2]^{3+}$ (2 mol%) and $SiO_2$/SPM:$[Eu(phen)_2]^{3+}$ (3 mol%). By optimizing these conditions, the relative efficiency value around 8% and 10% could be obtained, respectively. However, the reflectivity measured on the surface of coated a-Si PVC was ca. 7% higher than that of the non-coated PVC in the region from 330 to 800 nm. Therefore, it is expected to increase those outputs if the reflectivity is lowered by coating a low reflective film such as silica prepared by the sol-gel method.

# References


[1] S. Hufner, *"Optical Spectra of Transparent Rare Earth Compounds"*, Academic Press, New York, 1978.

[2] J. D. Main-Smith, *Nature*, **120**, 583 (1927).

[3] C. W. Struck and W. H. Fogner, *J. Lumin.*, **1,2**, 456 (1970).

[4] G. Blasse, *J. Chem. Phys.*, **45**, 2356 (1966).

[5] G. S. Ofelt, *J. Chem. Phys.*, **38**, 2171 (1963).

[6] S. P. Sinha, *"Complexes of the Rare Earths,"* Pergamon Press, London, England, 1966, P134.

[7] N. Flipescu, S. Bjorklund, N. McAvoy and J. Degnan, *J. Chem. Phys.*, **48**, 2895 (1968).

[8] S. P. Sinha, *J. Inorg. Nucl. Chem.*, **28**, 189 (1966).

[9] H. Samelson and A. Lempicki, *J. Chem. Phys.*, **39**, 110 (1963).

[10] G. Blasse, in K. A. Gschneider, Jr. and L. Eyling (eds.), *Handbook on the Physics and Chemistry of Rare Earths*, Vol. 3, North-Holland, Amsterdam, 1981, p.275.

[11] J.-G. G. Bunzli and G. R. Chopin (eds.), *Lanthanide Probes in Life, Chemical and Earth Sciences: Theory and Practice*, Elsevier, Tokyo, 1989.

[12] M. J. Weber, in K. A. Gschneider, Jr. and L. Eyring (eds.), *Handbook on the Physics and Chemistry of Rare Earths*, Vol. 4, North-Holland, Amsterdam, 1981, pp. 275-316.

[13] L. R. Matthews and E. T. Knobbe, *Chem. Mater.*, **5**, 697 (1993).

[14] N. Nelly, *J. Electrochem. Soc.*, **111**, 1253 (1964).

[15] W. Dew Horrocks, Jr. and M. Albin, *Progr. Inorg. Chem.*, **32**, 1 (1984).

[16] E. Banks, Y. Okamoto and Y. Ueda, *J. Appl. Polym. Sci.*, **25**, 359 (1980).

[17] W. M. de Azevedo, P. N. M. dos Anjos, D. L. Malta and G. F. de Sa, *J. Alloys Comp.*, **180**, 125 (1992).

[18] S. Sakka and K. Kamiya, *J. Non-Cryst. Solids*, **42**, 403 (1980).

[19] L. C. Klein, *The Glass Industry*, May 1982 and January 1981.

[20] E. T. Knobbe, B. Dunn, P. D. Fuqua and F. Nishida, *Appl. Opt.*, **29**, 2729 (1990).

[21] F. P. Schafer (ed.), *Dye Lasers*, Springer, Berlin, 2nd ed., 1977.

[22] B. Linter, N. Arfsten, H. Dislich, H. Schmidt, G. Philipp, and B. Seiferling, *J. Non-cryst. Solids*, **100**, 378 (1988).

[23] H. Schmidt and B. Seiferling, in *Mat. Res. Soc. Symp. Proc.*, **73**, 739 (1986).

[24] C. A. Capozzi and L. D. Pye, in *Proc. SPIE970*, p135, *Society of Photo-Optical* (Instrumentation Engineers, Bellingham, WA, 1988).

[25] H.-H. Huang, B. Orler and G. L. Wikes, *Macromolecules*, **20**, 1322 (1987).

[26] J. D. Mackenzie, *J. Sol-gel Sci. & Tech.*, **2**, 81 (1994).

[27] M. Yamane, S. Aso, and T. Sakaino, *J. Mater. Sci.*, **13**, 865 (1978) .

[28] D. Avnir, D. Levy, and R. Riesfeld, *J. Phys. Chem.*, **88**, 5956 (1984).

[29] K. Unger, *"Porous Silica,"* Elsevier, Amsterdam, 1979.

[30] A. I. McClellan and H. F. Harnsberger, *J. Colloid Interface Sci.*, **1967**, 577.

[31] C. J. Brinker and G. W. Scherer, *"Sol-gel Science,"* Academic Press, San Diego, CA, 1990, Ch. 13 and 14.

[32] S. Ikoma, S. Takano, E. Emoto, and H. Yokoi, *J. Non-Cryst. Solids*, **113**, 130 (1989).

[33] F. Orgaz and H. Rawson, *J. Non-Cryst. Solids*, **82**, 57 (1986).

[34] A. Makishima and T. Tani, *J. Am. Ceram. Soc.*, **69**, C72 (1986).

[35] A. H. Boonsta and T. M. N. Bernards, *J. Non-Cryst. Solids*, **105**, 207 (1988).

[36] S. Dire and F. Babonneau, *J. Sol-gel Sci. & Tech.*, **2**, 139 (1994).

[37] G. Philipp and H. Schmidt, *J. Non-Cryst. Solids*, **63**, 283 (1984).

[38] H. Schmidt, *J. Non-Cryst. Solids*, **73**, 681 (1985).

[39] R. Zusman, C. Rottman, M. Ottolenghi, and D. Avnir, *J. Non-Cryst. Solids*, **122**, 107 (1990).

[40] D. Preston, J. C. Pouxviel, T. Novinson, W. C. Kaska, B. Dunn, and J. I. Zink, *J. Phys. Chem.*, **94**, 2129 (1990).

[41] E. J. A. Pope and J. D. Mackenzie, *Mat. Res. Soc. Symp. Proc.*, **73**, 809 (1986).

[42] A. B. Seddon, C. A. Capozzi, S. L. Lana, T. A. King, X. Li, and G.-J. Gall, *J. Sol-gel Sci. & Tech.*, **2**, 181 (1994).

[43] T. M. Che, R. V. Carney, G. Khanarian, R. A. Keosian, and M. Borzo, *J. Non-Cryst. Solids*, **102**, 208 (1988).

[44] M. Laczka and M. Ciecinska, *J. Sol-gel Sci. & Tech.*, **3**, 219 (1994).

[45] T. Iwamoto, K. Morita, and J. D. Mackenzie, *J. Non-Cryst. Solids*, **159**, 65 (1993).

[46] M. Nakao, K. Itoh, T. Watanabe, and K. Honda, *Ber. Bunsenges. Phys. Chem.*, **89**, 134 (1985)

[47] N. Alonso-Vante, J.-F. Nierengarten, and J.-P. Sauvage, *J. Chem. Soc. Dalton Trans.*, **1994**, 1649.

[48] C. A. N. Fernando, *Sol. Ener. Mat. & Sol. Cells*, **30**, 211 (1993).

[49] K. S. Lim, M. Kanagal, and K. Takahashi, *J. Appl. Phys.*, **56**, 15 (1984).

[50] M. E. Langmuir, M. A. Parker, and R. D. Rauh, *J. Electrochem. Soc.*, **129**, 1705 (1982).

[51] A. Kay, R. Humphry-Baker, and M. Gratzel, *J. Phys. Chem.*, **98**, 952 (1994).

[52] N. Myung and S. Licht, *J. Electrochem. Soc.*, **142**, L129 (1995).

[53] T. Watanabe, T. Takizawa, and K. Honda, *Ber. Bunsenges. Phys. Chem.*, **85**, 430 (1981).

[54] R. Nakata, N. Hashimoto, and K. Kawano, *Jpn. J. Appl. Phys.*, **35**, L90 (1996).

# Acknowledgements

The author would like to express his heartfelt gratitude to Professor Dr. Gin-ya Adachi, Department of Applied Chemistry, Faculty of Engineering, Osaka University, for his continuous guidance, many invaluable suggestions, and his sincere encouragement thoughout the work.

The author would also like to thank Professor Dr. Gen-etsu Matsubayashi, Department of Applied Chemistry, Faculty of Engineering, Osaka University for his helpful comments and suggestions.

The author is deeply grateful to Associate Professor Dr. Ken-ichi Machida for his constant guidance and invaluable discussions, and Assistant Professors Dr. Nobuhito Imanaka and Hiroki Sakaguchi for their helpful advices and suggestions.

The author desires to express his sincere thanks to Professor Dr. Hiroaki Okamoto, Department of Electrical Engineering, Faculty of Engineering Science, Osaka University, Professor Dr. Shozo Yanagida, Department of Applied Chemistry, Faculty of Engineering, Osaka University, and all members of the research group of Professor Dr. Hiroaki Okamoto and Professor Dr. Shozo Yanagida, Osaka University for their kind guidance, helpful comments, and discussions on V-I characteristics measurements of the silicon PVC hybrid devices, and furthermore, Associated Professor Dr. Akifumi Onodera, Department of Material Physics, Faculty of Engineering Science, Osaka University, and all members of the research group of Associated Professor Dr. Fumiaki Onodera for their kind cooperation on this work.

The author wishes to thank Nichia Kagaku Inc. for supplying the standard phosphors $Y(P,V)O_4$:Eu and $LaPO_4$:Ce,Tb, and TDK Co., Ltd. for supplying the a-Si PVC.

Special thanks should be given to the author's co-workers, Mr. Shuji Tsutsumi, Mr. Yujiro Deguchi, and Mr. Satoshi Inoue for their helpful assistance and support in the course of this work, and all other members of the research group under direction of Professor Dr. Gin-ya Adachi, Osaka University, and to all of his friends for their help and friendships.

Finally, the author is particularly grateful to his parents Tetsumi and Kiyoko Jin, his grandmother Hagie Jin, and his brother and sister Hiroyuki and Akiko Jin for perpetual supports and continuous encouragements.